THE PENNSYLVANIA STATE UNIVERSITY
MILLENNIUM SCHOLARS PROGRAM

DEPARTMENT OF BIOLOGY

RESPONSE TO HIGH TEMPERATURE OF *CASSIOPEA XAMANCHANA* INFECTED WITH TWO DIFFERENT SYMBIONT TYPES.

GABRIELLE SWAIN
SPRRING 2018

A thesis
submitted in partial fulfillment
of the requirements
for a baccalaureate degree
in Biology

Reviewed and approved* by the following:

Dr Monica Medina
Associate Professor of Biology
Thesis Supervisor

Dr. Stephen Schaeffer
Faculty Title (Professor of Biology)
Reviewer

* Signatures are on file in the Millennium Scholars Program office.

ABSTRACT

The rise in sea surface temperatures has impacted marine ecosystems worldwide. In particular, significant damage has been observed across coral reefs due to bleaching, the breakdown of symbiosis between corals and its endosymbiont *Symbiodinium*. As the frequency of bleaching events continues to increase, so does the necessity to fully understand the mechanism of symbiosis breakdown. However, this can prove difficult due to the variation in response to temperature stress by different host-symbiont combinations. To determine the genetic response of temperature tolerant and intolerant symbionts to high temperature stress, we utilized the upside-down jellyfish *Cassiopea xamanchana* system. We infected *C. xamanchana* with two *Symbiodinium* clade A species: a temperature tolerant (KB8) and a temperature intolerant (EL1), and exposed the host to high temperature (32°C) to determine the changes in gene expression after 12 and 36 hrs. Under a single host context, we can determine how tolerance is conferred by different *Symbiodinium* types.

Table of Contents:

FIGURES:

TABLES:

ACKNOWLEDGMENTS

I'd like to thank the Medina lab for their patience throughout my 4 years in their lab. Thank you to Dr. Monica Medina, who brought me in as a freshman and showed me the joys of marine biology. Thank you to the graduate students in the lab who've helped me with difficult concepts and troubling experiments. Ana, Viri, and Sofia taught me so much, both about graduate level science and the life of a researcher. I'd like to offer special acknowledgments to Aki Ohdera, who was instrumental in the creation, execution, and publication of this project.

Special thanks to all those who have financed my research, including Penn State's SROP and REU program. Without these funds I would not be where I am today.

Lastly, I'd like to thank the Millennium Scholars program for pushing me to be the best scientist I can be.

CHAPTER I:
Introduction

Studies have suggested anthropogenic climate warming may have started as far back as the mid-19th century, as a result of the industrial revolution (Abram et al., 2016; Mann et al., 2008). The amount of carbon dioxide in the air has increased by 40% since the 1700s (Gossing et al. 2010). Increased production and subsequent accumulation of greenhouse gases such as carbon dioxide and methane are leading to higher absorption of heat and radiation.

Changes in thermal patterns caused by greenhouse gases have caused problems in biological systems. According to recent data published by NASA, the annual mean of earth's temperature has risen 1.0° C since 1880, with some models predicting another 3.0° C increase between 2050 and 2100 (IPCC 2007). In biological systems, higher temperatures induce shifts in natural systems relating to community structure, as well as seasonal and speciation patterns. Agriculturally, climate change has caused changes in the soil microbial community structure in field ecosystems (Gray et al. 2011). In addition to changing the nutrient and carbon cycling patterns, elevated temperature can affect the microbial enzyme activity and abundance. These factors are key processes involved in soil health, and therefore could negatively impact crop yields on multiple continents. Organisms of both terrestrial and marine origin have gone through significant change, specifically in species density at a given location, phenological tendencies, morphological components such as body size and behavior, and genetic frequencies (Parmesan and Yohe 2003). Newly introduced species pose a threat to native organisms, oftentimes outcompeting organisms and decreasing the ecosystem's biodiversity (Ward and Masters 2007). Spring events such as leaf unfolding, flower blooming date and migration patterns have all been shifted due to the non-traditional temperature increases (Root et al. 2003). These changes in

phenology cause confusion in the many precise niches found around the world. Altogether, climate change has and will continue to be a problem for organisms around the world.

Figure 1: Contrast between healthy (endosymbiont containing) and bleached corals (State of Hawaii 2017)

Scleractinian corals are organisms important in global ecosystem. Though corals serve many functions, reef building corals are important as biodiversity hotspots, providing an important habitat for many marine organisms, from algae to large fish. Corals can also be a source of high amounts of nutrients such as ammonia and phosphate, making them a safe haven within oligotrophic waters (Muscatine et al. 2005). Productivity within coral reefs can be 1000 times greater than surrounding areas (Hatcher 1990). Corals also provide protection to the coastline. Their rock-like structure provides a first-line defense against erosion and flooding by reducing the severity of waves crashing into the shore (Hughes et al. 2003). In these ways corals prove to be crucial in shaping and maintaining marine and coastal ecosystems.

Over the past 30 years, coral health has seen a sharp decline due to climate change (Gossing, et al. 2010). Coral cover has decreased dramatically, leaving fish without a location for feeding and creating nurseries. More than 75% of reef fish species have declined in abundance, with 50% declining to less than half their original number; at this rate, scientists believe most fish species will lose their habitats by 2050 (Jones et al. 2004). As more and more corals die, the biodiversity of coral reefs also decreases, reducing the overall health of the ecosystem.

Furthermore, many coral reefs are transitioning from a coral to algal dominated state (Hoegh-Guldberg et al. 2007). Shoreline health is also in decline, as increasingly brittle corals are unable to protect the coast from storm damage.

One of the biggest reasons for the decline in coral health is bleaching. Corals receive energetic benefits via an endosymbiotic relationship with the dinoflagellate algae in the genus *Symbiodinium*. The autotrophic *Symbiodinium* provide corals with their photosynthetic products (sugars and amino acids) in exchange for protection and nutrients. It is estimated that *Symbiodinium* provide around 95% of coral species' metabolic requirements (Hoegh-Guldberg 1999). Nitrogen, an essential and low abundance nutrient in oligotrophic waters, is closely regulated in the coral-*Symbiodinium* relationship, as the housing of the dinoflagellates provides a tight cycle. By encasing the *Symbiodinium*, corals decrease the susceptibility for nutrients like nitrogen to escape. The association is often fragile and *Symbiodinium* can be expelled due to high oceanic temperatures in a process called bleaching. The pigmentation largely attributed to coral reefs is lost, resulting in a white coloration after the symbionts are expelled. While corals may survive and recover after mild thermal stress, very rarely do they grow back as strong (Hoegh-Gudberg 1999). Oftentimes, a coral recovering from bleaching will grow back at a reduced rate with limited calcification and fecundity (Hoegh-Gudberg 1999). The largest global bleaching event occurred from 1997-1998, starting in the year now known as the International Year of the Reef. Reefs which had thrived the year before fell to the century's warmest El Nino and Indian Ocean Dipole (Donner et al. 2005). While small scale bleaching events were observed before 1998, this event was the first large scale bleaching event in recorded history, both in intensity and longevity (NOAA 1998). Coral bleaching can occur when sea surface temperatures increase by 1-2 degrees for more than three weeks. The temperatures during peak warming periods were about

1-2° C above long term means, and the waters with temperatures exceeding 30° Cinduced extensive coral damage for around 12 months (Donner et al. 2005). The Great Barrier Reef, widely known for its extensive range of colors and organisms, saw mortality rate as high as 80-90%. Across the globe, coral mortality rates ranged from 30-99%, ultimately leading to a complete change in the coral reef landscape (Hoegh-Guldberg et al. 2007)

While many scientists agree the rise in oceanic temperature has caused widespread bleaching events, not much is known about the mechanism behind *Symbiodinium* incorporation and maintenance in corals. If inferences regarding the effect of heat stress on symbiosis are to be made, a good understanding of cell biology must be known. The dinoflagellates are typically found within the host's inner most tissue layer and held in place via a mix of algal and host membrane (Davy, Allemand, and Weis 2012). The symbionts can be transferred vertically (directly from the parent coral) or can be incorporated post-embryogenesis. The establishment of the *Symbiodinium* occurs with an initial host-symbiont contact, followed by symbiont engulfment, and then an intracellular sorting of the symbionts within the host tissue (Davy, Allemand, and Weis 2012). Continued inhabitation occurs once the symbiont cells begin dividing and conclude with an establishment of stability between the host and symbiont. In the case of heat stress, the symbiotic association is disrupted, and ultimately broken down. While scientists know different signals allow host-symbiont recognition, the time frame regarding establishment and maintenance of symbiosis is still unclear. Current studies are investigating if a microbe associated molecular protein (MAMP) is needed only for establishment, or if it is also needed for maintenance of the symbiont (Davy, Allemand and Weis 2012). Perhaps the establishment and maintenance are not due to just one protein, but complex interaction between the symbiont with the host cell. A more detailed understanding of the processes involved in symbiont infection and continued inhabitation in a host

organism will create a better platform for relating environmental stressors to bleaching in cnidarians.

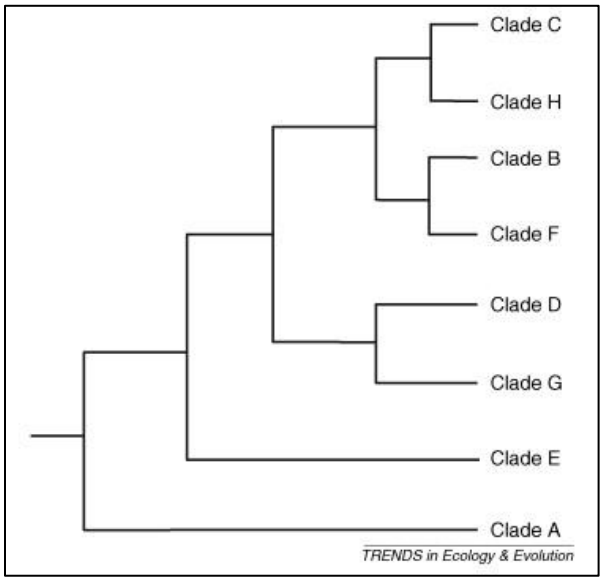

Figure 2: Relationship between the nine Symbiodinium clades (Weis et al. 2008)

Symbiodinium species contain a wide variety of physiological attributes, both within and between species. Originally, all symbiotic dinoflagellates were classified as *Symbiodinium microadriaticum* (Stat et al. 2008) However, studies performed in the 1980s started to reveal the diversity of *Symbiodinium* (Stat et. Al 2008). Current literature has identified 8 groups, or clades, within *Symbiodinium*. Clades A-H are classified based on their 18s rDNA nucleotide sequences, as their morphological features are too similar to use as clade distinguishers. Though clade E seems to only have one member, all other groups contain subclades with a wide variety of physiological properties. The physiological differences between *Symbiodinium* can also be translated to the host. Juvenile corals with Clade C *Symbiodinium* grow faster than corals with Clade D *Symbiodinium* but perform worse during times of thermal stress (Stat, Morris, and Gates 2008). While diversity between clades is common, there are also within-clade differences in physiology. For example, the aforementioned Clade C *Symbiodinium* have different subgroups that occur throughout the tropical zone. After breaking the zone down into subtropical and temperate regions, scientists found genetically different Clade C *Symbiodinium* subgroups based on their habitat location and temperature (Rodriguez-Lanetty, Krupp, and Weis 2004, Hume et al. 2013). Corals species like *Acropora hyacinthus* and *Pocillopora damicornis* contain a single

subgroup of *Symbiodinium* clade C in temperate water. However, this subgroup was found to be genetically distinct from the clade C *Symbiodinium* found inhabiting the subtropical populations of *Acropora* and *Pocillopora* (Lien, Fukami, and Yamashita 2013). Clade D has also garnered significant attention due to their physiology. This clade is a common type of *Symbiodinium* that is studied in heat stress experiments due to their variability in thermal tolerance (LaJeunesse et al. 2014). Clade D *Symbiodinium* can be found in higher than normal thermal environments, such as Palau, Thailand, and American Samao (Ladner, Barshis, and Palumbi 2012). The different *Symbiodinium* spp. are able to extend their physiological features to the host organism, potentially enabling the holobiont (*Symbiodinium* within a host organism) to cope with its environment.

Different approaches have been used to investigate the effect of environmental stresses, particularly thermal, on coral-dinoflagellate health. One noninvasive manner is to measure coral fluorescence during heat stress. Green fluorescent proteins (GFPS) are found inside the endosymbionts at high concentrations and are positively corelated with dinoflagellate photobiology. After exposure to thermal stress, the concentration and level of fluorescence decreased, as did the coral health, even before noticeable bleaching (Roth and Deheyn 2013). After bleaching, there was a strong level of fluorescence despite the reduced concentration of GFP found inside the corals (Roth and Deheyn 2013). The authors of this study concluded that GFP has a closer functional relationship to coral growth than to heat response and can be used as a physiological health measurement (Roth and Deheyn 2013). The photosynthetic properties of the reef building coral *Acropora digitifera* were also observed after heat exposure. This study began by speculating that a large portion of coral bleaching occurs due to the heat dependent photoinhibition of photosystem II and that bleaching is not due to the expulsion of symbiotic algae, but rather due to the photobleaching of the algal pigments, and subsequently, photosystem II

(Takahashi et al. 2004). The hypothesis of this paper states that corals fail to maintain their symbiotic relationship during heat stress because the repair system for the photodamaged PSII is inhibited by heat stress. The authors found that each coral species has their own heat susceptibility, and thus the efficiency of heat tolerance and bleaching susceptibility is variable.(Takahashi ET al. 2004). Gene expression via reverse transcription quantitative PCR was used in order to investigate the response of host genes when exposed to thermal stress. *Rhopaloeides odorabile* sponges underwent temperature induced necrosis to determine expression levels in each holobiont organism (Fan et al. 2013). The onset of elevated temperature showed immediate stress response in both communities, with a decrease in expression in genes relating to symbiosis maintenance. As nutrient exchange and molecular interactions decreased, so did the amount of infected symbiont cells in the host tissue until ultimately the symbiosis dissolved (Fan et al. 2013). Gene expression of key cellular processes was observed after exposing *Galaxea fascicularis* to heat stress using real time PCR. Of the 42,000 coral genes assembled, there was a significant upregulation in DNA integration and unfolded protein response (Lin et al. 2017). The authors speculate that high temperature activates the stress response at an early stage. Bleaching and lysing via DNA integration and unfolded protein response occurs after prolonged heat stress, as they are able to disrupt the symbiotic relationship between corals and dinoflagellates. Real time PCR can be used to measure gene expression during short term heat exposure in different functional coral species. *Stylophora pistillata, Acropora eurystoma*, and *Porites* species of corals were treated with thermal stress. The expression patters of seven genes relating to key cellular processes in heat-stressed cnidarians were investigated; these cellular processes included oxidative stress, Endoplasmic Reticulum (ER) stress, energy metabolism, DNA repair, and apoptosis. *A. eurystoma* was a susceptible coral species but did not show bleaching. However, redox genes were upregulated

early after thermal stress exposure. *S. pistillata* indicated an upregulation of stress markers before bleaching, and the genes remained highly expressed or decreased slightly once surrounding temperatures reached 34° C, while *Porites* bleached at a lower temperature (32° C), and the stress marker genes only significantly increased in expression at bleaching temperature (Maor-Landaw and Levy 2016). The authors postulated that the expulsion of symbionts from *Porites* tissue reduce the oxidative damage placed on the host, and the stress genes only present themselves at bleaching.

Heat shock proteins have been used to measure the level of cellular response in thermally stressed individuals (Clark et al. 2008, Aruda et al.2011, Park and Kwak 2014). Organisms have evolved to express these small proteins and will use the metabolic adjustment process in order to maintain cellular homeostasis. (Kotak et al., 2007; Mittler at al., 2012). One study in particular used transcriptomics to understand how heat proteins played a role in response of *Pocillopora damicornis* to environmental changes using RNAseq (Zhang et al. 2018). The investigators identified heat stress protein 70 as a potential player in the regulation of corals in thermal stress based on previous literature. They then discovered a form of HSP 70, PdHSP70 in their differentially expression analysis. They speculated that the expression was induced by elevated temperature and ammonium levels. Though genetic expression increased significantly after 12 hours, PdHSP70 expression returned to normal levels after 24 hours of thermal stress. Enzyme activity was observed in PdHSP70, and it was determined that levels remained stable throughout the increase in thermal temperature. The authors concluded that as the PdHSP 70 mRNA can be induced by diverse environmental stressors including heat, and the activity of the protein remains stable, regulating the host-response to heat stress (Zhang et al. 2018). Oxidative stress genes and heat shock proteins are common markers to measure thermal stress in marine organisms. A recent study set out to evaluate which marker works better in quantifying heat stress in the coral species

Porite astreoides. Infected samples were exposed to ambient (27.3°C) or elevated (30.8° C) temperatures for 4, 24, and 48 hours. The study found elevated temperature had no effect on larval survival, settlement, or expression of HSP 16 or 60. However, elevated temperature caused significant increase in larval respiration, oxidative damage, and antioxidant enzyme activity. The absence of significant up regulation of heat shock proteins in response to thermal stress indicate a decreased sensitivity in reporting the effects of heat stress on corals. Therefore, the authors conclude that the enhanced levels of oxidative stress markers expressed during the experiment justify its use as the preferred method of heat stress measurement in coral species.

As stated previously, a large part of coral health lies in the molecular underpinnings its symbiotic relationship. Instead of using corals, scientists have proposed using model organisms to investigate bleaching for increased efficiency and transparency. These model organisms are easier to maintain in the lab (fast growth rate, small size, and hard to kill), and have clear molecular benefits (clonal populations, easily manipulated, and visible microscopy analysis) (Davy, Allemand, and Weis 2012). Recently scientists have used model organisms such as *Exaiptasia pallida* and *Cassiopea xamachana* to investigate cnidarian-*Symbiodinium* symbioses during heat stress (Perez and Weis 2006, Cabrales-Arellano et al. 2017). Found mainly in the Caribbean and along the Florida Keys, the upside-down jellyfish *C. xamachana* is native to tropical and subtropical areas. Like corals, they establish an endosymbiotic relationship with *Symbiodinium*, allowing nutrient exchange between the two organisms. The jellyfish are commonly found living in shallow depths, as light is important for the autotrophic *Symbiodinium* species living inside the organism. One of the main advantages of *Cassiopea* is their ease of maintenance and upkeep in the laboratory for efficient experimental manipulation (cite Aki's recent review paper). Aposymbiotic polyps (individuals without *Symbiodinium*) can be exposed to different clades of

Symbiodinium in the laboratory, which allows for comparative studies using a single host context. Symbionts can be lost in the jellyfish much like corals due to increases in environmental temperature. While *Cassiopea* are fairly temperature tolerant, prolonged exposure to heat stress (at least 2° higher than average for ≥ 3 weeks) will cause *Symbiodinium* expulsion from the host tissue (Hoegh-Guldberg 1999). Recent advancements in resources for *C. xamachana* as a model organism to study cnidarians-dinoflagellate symbiosis has provided a critical opportunity to address new questions. We have been able to create clonal laboratory lines of *Cassiopea xamachana*, thereby controlling the genetic variability between samples. Furthermore, recent advances in genomics tools allow for the drafting of transcriptomes and genome assemblies, making it easier to evaluate differentially expressed genes during environmental stress.

This paper evaluates the effect of heat stress on *Cassiopea xamachana* using RNAseq. Temperature, *Symbiodinium* species, and incubation period can affect the gene expression in juvenile *Cassiopea xamachana*. Two clade A types, one heat-intolerant (EL1) and another heat-tolerant (KB8) were used to infect apo-symbiotic jellyfish. The jellyfish were incubated for either 12 or 36 hours in 26° and 32° C environments. Using next-generation Illumina sequencing, we were able to sequence the transcriptomes and compare gene expression of the host infected with physiologically different symbionts. Based off data from previous studies involving corals and other model cnidarians, we believe there EL1 will be unable to aid its *Cassiopea* host during prolonged heat stress, thereby causing the *Cassiopea* to express a higher amount of stress related DEG than the heat tolerant group (KB8-infected).

CHAPTER 2:
METHODOLOGY

I. MATERIALS

The *Cassiopea xamachana* samples were taken from the established farm in the Medina Lab at Pennsylvania State University. Senior members of the laboratory collected samples from the Florida Keys and brought back to the lab. Aposymbiotic larvae were grown into aposymbiotic polyps and kept in a separate section of the lab to avoid accidental infection with *Symbiodinium*. The polyps were fed with *Artemia* brine shrimp twice a week and cleaned with laboratory created sea water. Uninfected polyps were kept at 26° Celsius and separated based on their line. The lab maintains 3 out of the 12 lines (T1, T2, T3) ranging from type A-F.

II. EXPERIMENTAL DESIGN

Uninfected TIE (n=6), T1F (n=7), and T2E (n=5) lines of *Cassiopea xamachana* polyps were taken from the apo-polyp farm for infection. As stated previously, the *Cassiopea* lines are a part of the clonal population various labs have used to increase transferability between model organism studies. Particularly, these three lines were chosen from the set due to their analytical power. Comparisons can be made between the *Symbiodinium's* effect on both line (T1 vs T2) and type (E or F) of the host organisms. *Symbiodinium* types from clade A were introduced to the polyps during feeding. KB8 (A1) was chosen because of its popular infection in *Cassiopea*, as well as its heat-tolerance properties. EL1 (A3) can also be found in natural symbiotic relationships but has shown less tolerance when exposed to heat. As both *Symbiodinium* types belong to clade A, they could provide information about the inner-type diversity of *Symbiodinium* types. *Cassiopea* polyps

were incubated at 26 ° C to allow proper infection of their symbiont. An average oceanic temperature of 26 ° is common for the *Cassiopea* found in the Florida Keys, and was therefore set as a control temperature for the experiment.

A warm environment (32° C) was added to the experiment once polyps matured into ephyra (a sign of successful infection with *Symbiodinium*). Lab members determined that corals and *Cassiopea* could survive at this temperature but showed signs of stress as time progressed. Six samples (3 KB8 infected, 3 EL1 infected) were placed into the control environment while the other 12 samples (6 KB8 infected, 6 EL1 infected) were placed in the warm condition. The samples were incubated for either 12 or 36 hours before RNA extraction

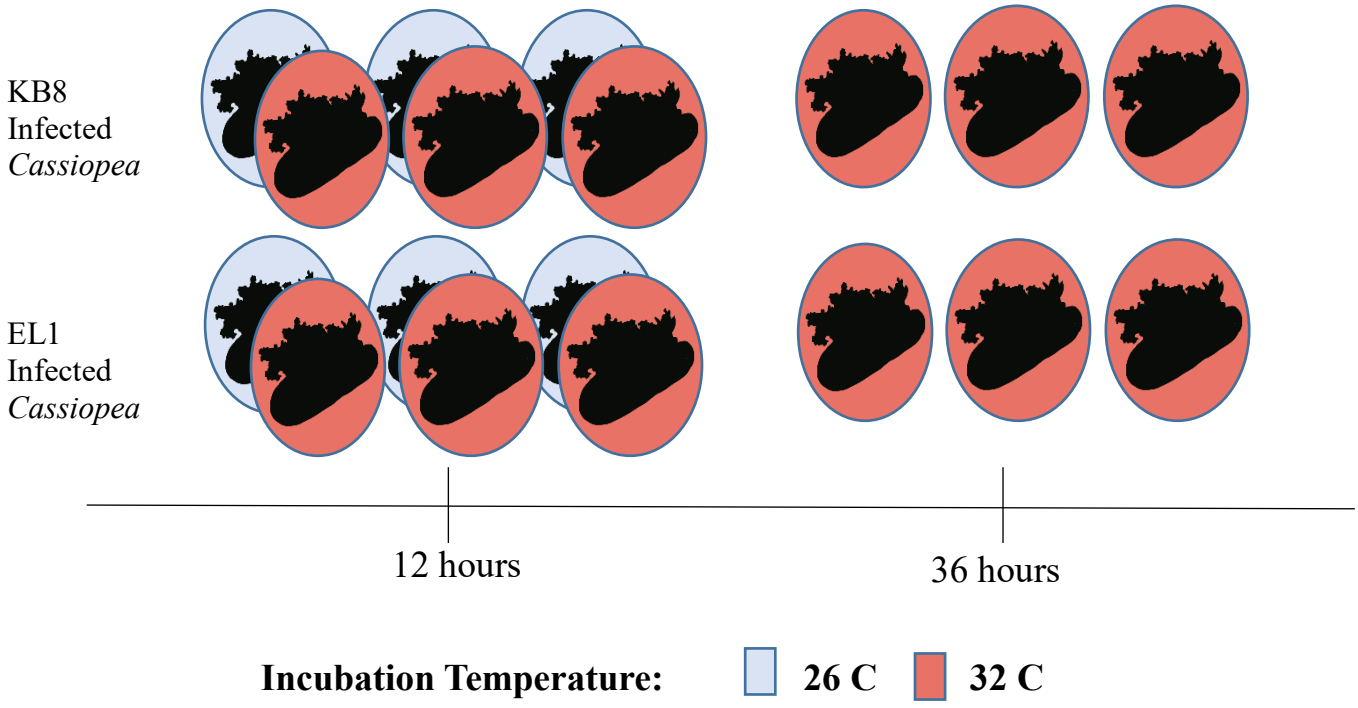

Figure 3: Experimental Design

Cassiopea Line	*Symbiodinium* type	Temperature of Incubation (C)	Time of Incubation (hr.)
T1E	EL1	26	12
T1F	EL1	26	12
T2E	EL1	26	12
T1E	EL1	32	12
T1F	EL1	32	12
T2E	EL1	32	12
T1E	EL1	32	36
T1F	EL1	32	36
T2E	EL1	32	36
T1E	KB8	32	12
T1F	KB8	26	12
T2E	KB8	26	12
T1E	KB8	26	12
T1F	KB8	32	12
T2E	KB8	32	12
T1E	KB8	32	36
T1F	KB8	32	36
T1F	KB8	32	36

Table 1: A list of the samples used in the RNAseq analysis broken down by experimental condition

III. RNAseq ANALYSIS

Eighteen samples were made into cDNA libraries and sequenced using Illumina HiSeq. Reads were rid of contaminants and low-quality reads by use of Trimmomatic (YOU SHOULD ADD THE CITATION FOR YOUR SOFTWARE) before the analysis. In Trinity (REF), a *Cassiopea* draft genome was used to guide the transcriptome assembly. The indexing, alignment of the reference library was done using bwa (REF). Bwa was used again to map the RNASeq reads of each sample to the reference genome. The samples were converted into bam files and indexed using samtools (REF). The text files were made using samtools and concatenated into two files using Command Line (KB8 and EL1).

IV. DEseq ANALYSIS

R was used to analyze the up or down regulation patterns of the samples. A DEseq (REF) analysis procedure was modified to fit the experimental conditions. The search was to determine what, if any, genes occurred in multiple samples, and across different types. A type-based DESeq was performed to determine the DEG in same-type infections (i.e analysis of 9 EL1 samples only) followed by an overarching analysis (analysis of all 18 samples. A pairwise comparison was performed within same-type infections to ensure an-in depth understanding of heat stress processing. The comparisons in same-type infections used time and temperature as the variables of interest. Analysis was done on both concatenated files with various parameters with an icolno of 9 used for both files. This measure was performed to decrease the number of low-count reads interfering with the analysis, ensuring higher quality results. Either temperature or time of incubation was used as the treatment of comparison found at the end of the DESeq dataset. The control conditions were set as follows: T1E for line, 26°for temperature, and 12 hours for time. The DESeq was then run as a Wald's test to determine if the selected variable was significant in the model. Based on the previous research and papers published, time and temperature were the main variables tested in the model. After a size factor was added, the 3-way interaction table and MA-plot was created to visualize the effect

of the variable. Summaries of all combinations were made in R and then reported in an excel spreadsheet. CSV files were made from each DESeq and used for BlastX protein searches.

CHAPTER 3:
RESULTS

I. DESeq Analysis

The pairwise function was used in R to generate the differentially expressed genes.

KB8:

Control vs Short Term Heat Stress: The comparison was between KB8-infected *Cassiopea* incubated for twelve hours in 26° and 32° C environments. Of the 332142 genes with a nonzero total read count, 28 (0.0084%) genes were down-regulated and 51 genes (0.015%) up-regulated. There were 467 outliers (0.14%) and 251016 low counts (76%), with a mean count below 29. Of the down-regulated genes, there was a range of log2FoldChange between -2.47675 and -1.31944, while the up-regulated genes ranged from 4.320707 to 0.931574.

Control vs. Long Term Heat Stress: The comparison was between KB8-infected *Cassiopea* incubated at high temperatures (32° C) for 36 hours and the control parameters (12 hours at 26° C). Of the 133 genes with a nonzero total read count, 102 (77%) genes were down-regulated and 31 genes (23%) up-regulated. There were no outliers or low counts, and the mean count was below 29. Of the down-regulated genes, there was a range of log2FoldChange between -4.213719 and -1.95242, while the up-regulated genes ranged from 3.3779382 and 0.8980797.

Short vs. Long Term Heat Stress: The comparison was between KB8-infected *Cassiopea* incubated at high temperatures (32° C) for 12 and 36 hours. Of the 88 genes with a nonzero total read count, 84 (95%) genes were down-regulated and 4 genes (4.5%) up-regulated. There were no outliers or low counts, and the mean count was below 45. Of the down-regulated genes, there was a range of log2FoldChange between -4.267391667 and -1.172339585, while the up-regulated genes ranged from 1.3426372 to 0.7353787.

EL1:

Control vs Short Term Heat Stress: The comparison was between EL1-infected *Cassiopea* incubated for twelve hours in 26° and 32° C environments. Of the 390 genes with a nonzero total read count, 240 (62%) genes were down-regulated and 150 genes (38%) up-regulated. There were no outliers or low counts, and the mean count was below 40. Of the down-regulated genes, there was a range of log2FoldChange between -10.35637 and -1.179938, while the up-regulated genes ranged from 3.2766148 to 1.2293128.

Control vs. Long Term Heat Stress: The comparison was between EL1-infected *Cassiopea* incubated at high temperatures (32° C) for 36 hours and the control parameters (12 hours at 26 C). Of the 426 genes with a nonzero total read count, 132 (31%) genes were down-regulated and 150 genes (69%) up-regulated. There were no outliers or low counts, and the mean count was below 1. Of the down-regulated genes, there was a range of log2FoldChange between -12.48912 and -1.323385, while up-regulated genes ranged from 7.5193117 to 1.8592549.

Short vs. Long Term Heat Stress: The comparison was between EL1-infected *Cassiopea* incubated at high temperatures (32° C) for 12 and 36 hours. Of the 2533 genes with a nonzero total read count, 731 (29%) genes were down-regulated and 1802 genes (71%) up-regulated. There were no outliers or low counts, and the mean count was below 17. Of the down-regulated genes, there was a range of log2FoldChange between -4.267391667 and -1.172339585, while the up-regulated genes ranged from 1.3426372 to 0.7353787.

***DEG Patterns*:** A complete list of annotated genes for the experiment can be found in Appendix I. Of the genes, heat shock proteins and peptidyl isomerases were the only two consistently presented in both EL1 and KB8 infected *Cassiopea* in response to heat stress. Heat shock proteins (HSPs)

had the highest occurrence of differentially expressed genes (35 instances) for the experiment. Ranging from 7 to 110, the HSPs were mostly downregulated in KB8-infected comparisons (11 genes) and upregulated in EL1-infected samples (21 genes). Breaking down the distribution further, a majority of differentially expressed HSPs in EL1-infected samples originated from the control vs. short term heat stress and the short term vs. long term heat stress comparisons. In contrast, KB8-infected samples were had differential expression of HSPs in the control vs. short term heat stress and the short term vs. long term heat stress comparisons. Peptidyl isomerase is even more specific, as the gene was only upregulated in EL1 (4 times) and downregulated in KB8 (2 times). Some genes like serine-arginine rich splicing factors and high mobility proteins were only downregulated with the majority being expressed in the control v. heat stress comparisons. There was some specificity in DEG, as both EL1 and KB8 infected *Cassiopea* expressed unique genes for their infection. *Cassiopea* with EL1 differentially expressed cytochrome p450 proteins at high rates (11 upregulated, 3 downregulated) while protein disulfides were specific to KB8-infected *Cassiopea* (5 downregulated). Other EL1-infected proteins include downregulated proteins coactosin and angiotensin, and upregulated calcyclin and ubiquitin.

II: DESeq2 Results:

4A:

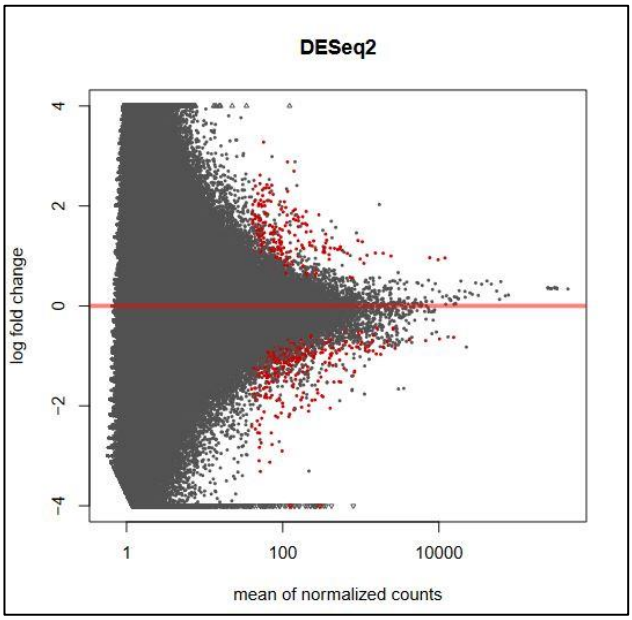

4B

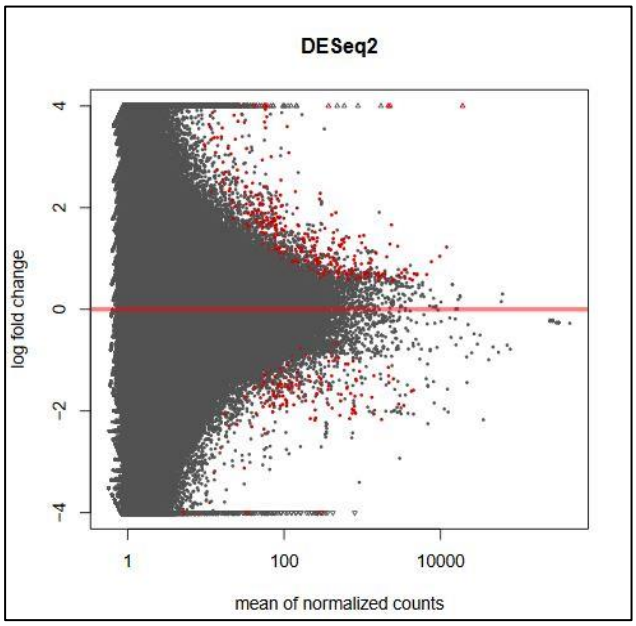

4C

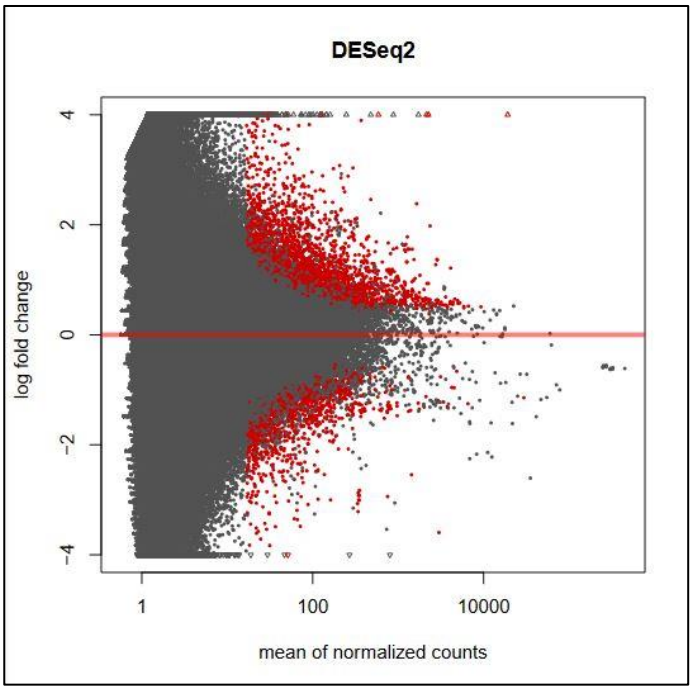

Figure 4: MA plots of EL1-infected Cassiopea.

MA plots of EL1-infected *Cassiopea* showing the log2 fold change for pairwise comparisons over the average of counts normalized by size factors. Grey dots indicate total normalized differentially expressed gene, red dots indicate genes with an FDR (False Discovery Rate) value below threshold. **A**: 12 hours at 26° C vs. 12 hours at 32° Celsius. **B**: 12 hours at 26° C vs 36 hours at 32° Celsius. **C**: 12 hours at 32° C vs 36 hours at 32° Celsius.

DESeq2 MA plots were generated based on the 18 libraries in a pairwise fashion. EL1-infected comparisons had a large base, indicated a broad range of log2foldchange (-4 to 4) with lower means (around 1-50). Genes below FDR appeared upwards of an 80-mean count for 4A, 50 for 4B, and 75 for 4C.

4A:

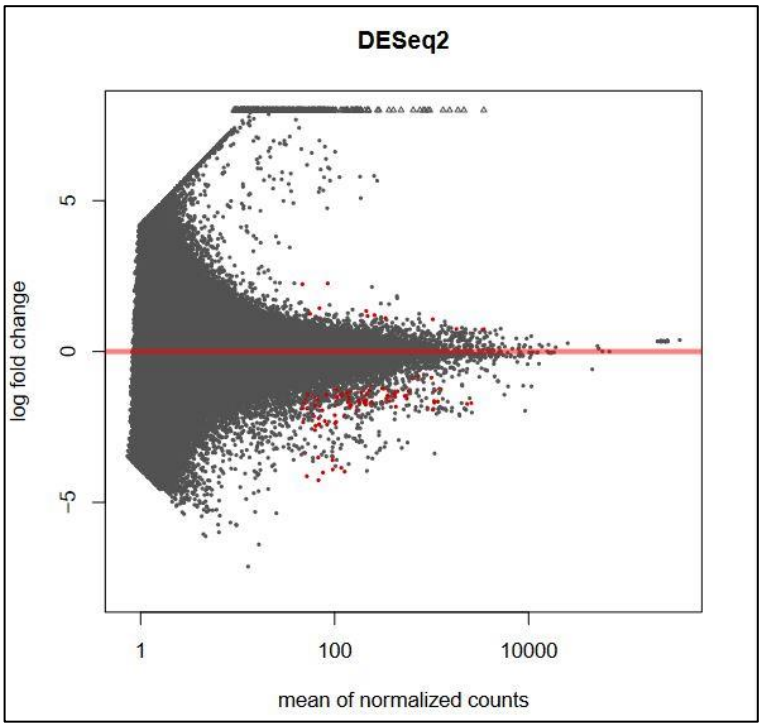

4B:

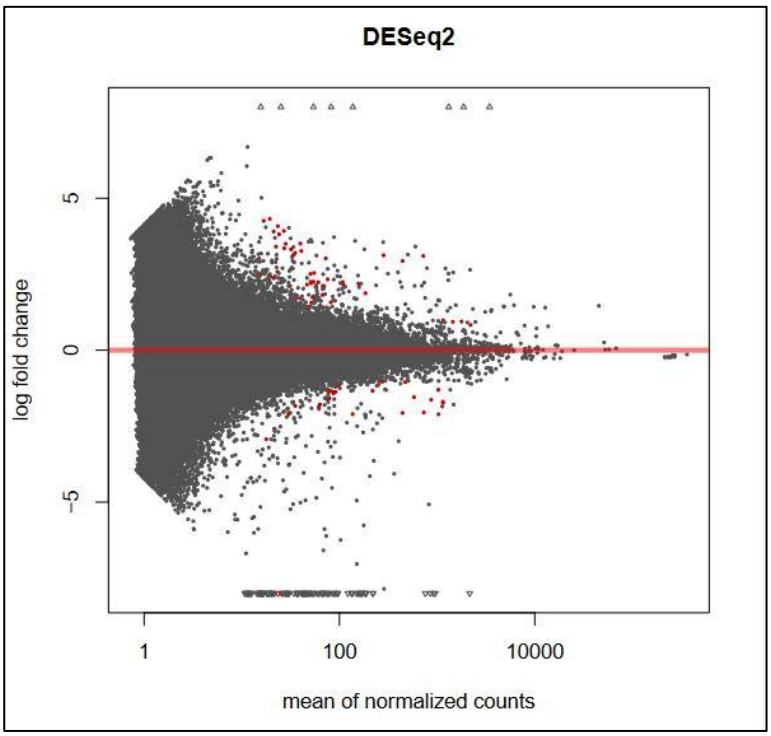

4C:

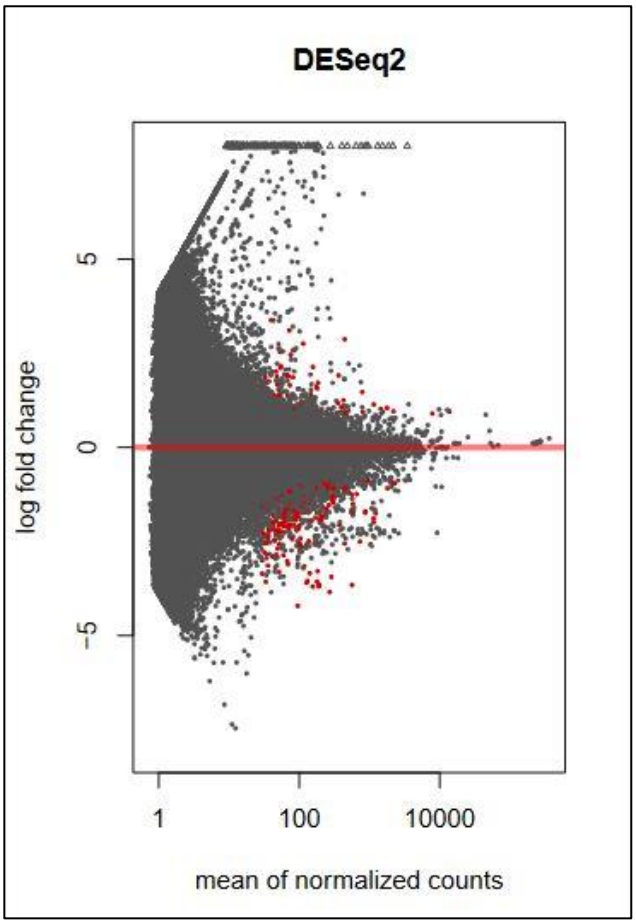

Figure 5: MA plots of KB8-infected Cassiopea

MA plots of KB8-infected *Cassiopea* showing the log2 fold change for pairwise comparisons over the average of counts normalized by size factors. Grey dots indicate total normalized differentially expressed gene, red dots indicate genes with an FDR (False Discovery Rate) value below threshold. **A**: 12 hours at 26 C vs. 12 hours at 32 Celsius **B**: 12 hours at 26 C vs 36 hours at 32 Celsius. **C**: 12 hours at 32 C vs 36 hours at 32 Celsius.

KB8-infected comparisons had a large base, indicated a broad range of log2foldchange (> -5 to 5) with lower means (around 1-30). Genes below FDR appeared upwards of an 80-mean count for 4A, 50 for 4B, and 90 for 4C.

III: ClusterProfiler

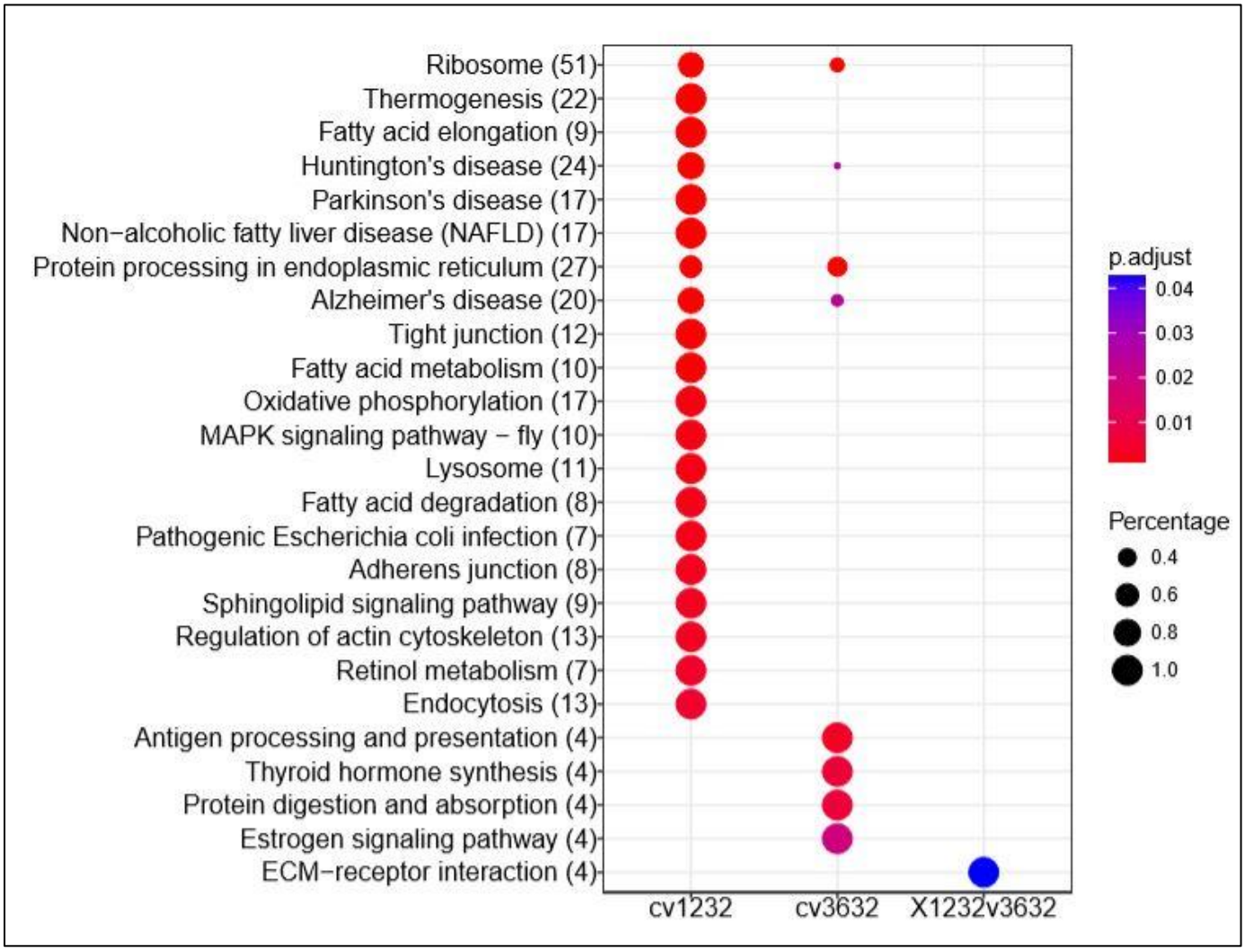

Figure 6: EnrichKEGG of EL1-infected pathways

Comparison of GO enrichment of gene clusters. The x-axis labels the sample comparisons used (Control vs 12hrs32°, control vs 36hrs32°, and 12hrs32° vs 36hrs32°). The color of the dots represents the range of P values, while the size of the dot shows the percentage at which the pathways was upregulated.

Proportions of popular KEGG pathways were found in the Cluster Profiler analysis between pairwise comparisons in EL1. The gene group containing the control vs. short term heat stress (control v 12hr 32°C) had the highest enrichment of the three contrast groups, while the short-term vs long term heat stress pairing (12hr 32°C v 36hr 32°C) had the least enrichment. Overlap between enriched pathways occurred between control v 12hr 32°C and control v 36hr 32°C groups (Figure 6). These processes included: Alzheimer's disease, protein processing in the endoplasmic reticulum, Huntington's disease, and the ribosome pathway. No pathways were expressed at enriched values across the three gene groups.

CHAPTER 4:
Discussion and Conclusion

Based on the data presented above, the hypothesis can be accepted; the *Cassiopea* samples infected with heat intolerant EL1 were more sensitive to an increase in temperature, as seen in the comparatively larger differential expression of stress-related genes than in KB8-infected samples. The various cellular states induced in the samples, including oxidative stress, ER stress, chaperone activity, and apoptosis all hint at the role of symbiosis in an increased oceanic temperature.

I: KB8-infected *Cassiopea*

The major processes connected to the differentially expressed genes in this group were related to stress, DNA damage, and apoptosis.

The pairwise comparison of 12 hours at 26 degrees vs 12 hours at 32 yielded very little DEG, both up and down regulated, connecting to stress or damage. Glycine-rich RNA binding protein was downregulated, and it has been linked to abiotic stress function in other organisms (Kim et al 2007). High mobility group B protein 2 was also downregulated in the control vs short term heat stress group. High mobility proteins have been shown to be involved in DNA damage control, ultimately leading to apoptosis (Fujikane et al. 2016). Regulated and scheduled cell death is important during times of stress, as this process keeps the organism safe from unwanted cellular waste, including damaged cells (Kannan and Jain, 2000). Therefore, processes regulating apoptosis determine the integrity of the cellular population. Of the upregulated genes, only a heat shock protein (HSP 83 fragment) and a peroxisomal targeting signal 2 receptor showed promise in relation to stress, as both have links to oxidative stress regulation (Schrader and Fahimi 2006), Neta-Sharir et al. 2005). As mentioned previously, heat stress proteins are expressed in organism

as a regulatory mechanism to fight environmental stressors (Benjamin and McMillan 1998, Rajan and D'Silva 2009, King and MacRae 2015). Exposure to abiotic stress usually result in protein damage and therefore dysfunction; heat shock proteins prevent the aggregation of damaged or misfolded proteins and ensure a healthy population of functional proteins in a cell. The chaperone activity may also include protein refolding under stressful conditions. Therefore, heat shock proteins will return a stress-induced cell into a state of homeostasis if the stress is not too great. Peroxule formation is another process which plays a key role in regulating stress perception and cell response when exposed to environmental cues. A larger logfold2change in the up-regulated genes (3.4 and 2.2) suggest a higher involvement in the heat stress response compared to the down-regulated genes (-2.1 and -1.37). Given the annotations and amplitudes of this group's DEG and the shorter incubation of thermal stress, the KB8-infected *Cassiopea* seemed to be preparing for an increase in cellular response.

DEG in the pairwise comparison of 12hr26° vs 36hr32° showed higher annotation of down-regulated genes relating to stress and damage. Possible oxidative stress genes in the downregulated DEG results include dual oxidase 1(-3.6 log2FoldChange), Eosinophil peroxidase (-3.0 log2FoldChange), and Collagen alpha -1 chain (-1.3 log2FoldChange). Overexpression of dual oxidase 1 has been proven to increase the concentration of reactive oxygen species (ROS), ultimately leading to oxidative stress in a cell (Sandiford et al. 2014). Eosinophil peroxidase (EPO) increase the cellular level of oxidative stress to the point of apoptosis in the organism (Salunga et al. 2007). In an autotrophic organism, oxidative stress refers to anything which causes the strain, damage, or death of its chloroplasts. Any harm which befalls the chloroplasts has a large-scale effect, as a damaged chloroplast cannot make as much energy via photosynthesis. Another protein of interest, Collagen has been proven to be signaled by oxidative stress in order to regulate the cell

(He et al. 2015, Sahu et al. 2017). As an antioxidant response mechanism, heat shock proves dangerous, as past research has shown how heat damage can increase the breakdown of collagen, thereby weakening the overall system (Park and Oh, 2015). Another phenomenon observed was endoplasmic reticulum stress. One of the largest symptoms of ER stress is apoptosis, or cell death. Translocon-associated protein subunit gammas with log2FoldChanges of -1.7 and -1.2, and a protein disulfide isomerase A5 with a value of -1.33 have been linked to extreme ER stress resulting in apoptosis (Chen et al. 2013, Dunlop et al. 2018). Though not as substantial, the up-regulated DEG provide further proof for this theory. Uromodulin (1.9) is involved in ER stress regulation and cell death while NADPH-dependent aldo-keto reductase (1.2) is produced in response to oxidative stress (Allison 2017, Endo et al. 2009). High mobility proteins and abiotic stress genes were differentially expressed as well (both up and down-regulated) in this group, suggesting the transition from preparation to execution of cellular response after long term thermal stress. Therefore, though the host is showing signs of heat stress, additional cellular processes are adequate to cope with the stress.

The pairwise comparison between 12hrs32° and 36hrs32° showed the highest amount of DEG relating to heat stress, DNA damage, or ER stress. A majority of the down-regulated annotated genes are linked to heat stress (6 annotations) or ER stress (11 annotations). Heat Shock Proteins 7, 9, 18, 94 were all downregulated, with a downregulation of 7 and 9 appearing twice. Heat shock protein 7 associates with heat shock 70, one of the most studied groups in thermal stress studies, while HSP 9 appears during general abiotic stress (Chan 2015, YE 2012) HSP 90, the other popularly studied heat shock protein, was proven to associate with both 7 and 9 during thermal stress (Saito et al. 2015). In terms of ER stress, there were multiple appearances of disulfide isomerase A4 (4) and calreticulin (3) and mesencephalic astrocyte-derived neurotropic factor

homologs (2). Unfolded protein during ER stress have been shown to interact with calreticulin to mediate damage to the cell, while mesencephalic astrocyte-derive neurotropic factors are mainly used as biomarkers for ER stress in organisms (Vargas 2016, Kim et al. 2016). The only upregulated gene of note was a DNA homolog subfamily C member, which has links to ER stress as well. However, the log2foldchange was lowest of the annotated genes (0.7) and did not contribute as much to the cellular environment. Therefore, as most of the stress-related DEG are downregulated, the data could indicate a return to a stable cellular environment in KB8-infected *Cassiopea* sometime between 12hrs and 36hrs after exposure to thermal stress.

II: EL1-Infected *Cassiopea*

Based on the DEG results, EL1 infected samples did coincide with similar cellular processes as KB8 throughout the heat stress experiment. While each of the three comparisons showed links to oxidative stress, heat shock protein regulation, ER stress and DNA damage, the severity of the up or down regulation was increased in the EL1 samples.

The pairwise comparison of 12hrs26° and 12hrs32° mainly showed signs of oxidative stress, DNA damage and apoptosis. Down-regulated genes relating to apoptosis and protein refolding scored higher on the log2FoldChange scale, while most heat shock proteins and oxidative stress genes had smaller scores. Serine/arginine-rich molecules appeared twice in the down-regulated data (log2FoldChange of -3.1 and -2.8), suggesting a high influence on the samples. Past literature has linked this splicing factor to protein refolding, specifically after ER stress was observed in the organism (Dunlop et al. 2018). Additional chaperone activity was inhibited via the downregulation of an activating chaperone transcription gene and COMM domain-containing protein 5. The high

mobility group proteins were downregulated, showing links to apoptosis regulation in this comparison as well. One abiotic stress-related protein (glycine-rich RNA-binding protein 2) was downregulated, indicating only a slight role in the cellular processes. Oxidative stress was expressed moderately in the analysis (-2.24 and -1.4). The largest oxidative stress logfold2change was for a tyrosinase molecule, which past studies have shown to be associated to oxidative stress levels (Eskandami et al. 2010). Quinone oxidoreductases role is to translocate NADH and sodium, but also has been proven to enhance oxidative stress in organisms (Muras et al. 2016). The data suggest a decrease of cellular activity devoted towards DNA and protein modification as thermal stress begins to damage the cellular environment. The up-regulated genes in these data set provide evidence for this theory. All annotations relating to possible environmental stress regulation were either related to oxidative stress of chaperone activity. Specifically, most of the oxidative stress genes related to cytochrome P-450 molecules, and chaperone activity due to heat shock proteins. Cytochrome p450 enzymes break down potentially toxic compounds like reactive oxygen species (Narusaka et al. 2004). Heat shock proteins 40, 60, 70, 90 and 105 were differentially expressed, as well as a HSP70-90 organizing protein. Peptidyl-prolyl cis-trans isomerase appears in multiple pathways, including oxidative stress and heat tolerance. As stated before, HSP 40 works as a co-chaperone with HSP 70 to promote proper protein folding. HSP 60 works at a later stage, as it promotes apoptosis in a cell (Kim et al. 2009). HSP 70 and 90 are of particular note due to their implication in heat stress regulation through chaperone activity (Chen et al. 2014). Like previous studies, our data suggest upregulation of these proteins in multiple locations. It is probable therefore that the large while molecules dealing with oxidative stress and DNA misfolding were downregulated, the samples were attempting to reverse the damage via chaperone proteins like HSP and cytochrome p450.

Differentially expressed genes between 12hrs26° and 36hrs32° were focused on oxidative stress, chaperone activity, and apoptosis. While there were some re-occurring, genes appearing in the down-regulated results, a majority of the annotated genes had links to oxidative stress, and possible connections to chaperone activity. High mobility proteins were downregulated again, as was a glycine-rich RNA binding protein. Collagen alpha expression was downregulated nine times in the data set. At such a high rate, it can be deduced that the level of oxidative stress is severe during the 24 hours of thermal stress occurring in this comparison. Evidence for high levels also comes from the appearance of angiotensin-converting enzymes in the down-regulated results. Research has found that Angiotensin-converting enzymes (ACE) will be inhibited during times of oxidative stress (Reza et al. 2016). The inhibition of these two molecules suggests a state of high oxidative stress once left in a warm environment for more than 12 hours. The up-regulated genes were similar to that of the previous comparison: mainly genes involved in chaperone activity, and minimal amounts related to oxidative stress. Heat shock proteins 7,9,18 67, and 71 were expressed at elevated rates. Once again, the high levels of chaperone activity could suggest high amounts of cellular stress, possibly in the form of oxidative stress. Further evidence can be found in the up-regulation of peptidyl-prolyl cis-trans isomerase and Y+L amino acid transport genes, as both are linked to oxidative stress response (Hong et al. 2002, Yin et al 2005).

Contrastingly, the comparison between the two heat stress groups (12hrs32° vs 36hrs32°) had the least amount of differentially expressed genes in the EL1 dataset. Most of the down-regulated DEGs seem only to appear in differentially expressed levels during stress. Chitinase 1, and the related chitotriosidase, are inhibited during times of stress to increase the tolerance (Takenaka et al. 2009). The only other stress-related gene in the downregulated data set was a zinc finger RNA-binding protein, which can be induced during times of stress, and can confer abiotic stress tolerance

(Tran et al. 2007, Giri et al. 2011). The overall log2FoldChange for chitinase was about three times higher than zinc's (Figure 7B), indicating a higher significance of stress tolerance. This holds true for a portion of upregulated genes. Beta, beta carotene 15' and 9' were upregulated at high logFold2change values (4.9 and 4.9) and are thought to reduce oxidative stress in an organism (Kaspercyzk et al. 2014). Other upregulated genes had connections to oxidative stress, and oxidative stress-induced apoptosis. Dual oxidase had the highest log2Foldchange (7.7) and has been found to increase the concentration of reactive oxygen species in a cellular environment (Sandiford et al. 2014). Eosinophil peroxidase, the second highest log2Foldchange value (7.7) is involved in oxidative stress induced apoptosis (Salunga et al. 2007). Upregulated genes with smaller log2Foldchange values such as Uromodulin, Methionine synthase, and e3 ubiquitin protein ligase add evidence towards the claim that prolonged heat stress in EL1 leads to oxidative stress and ultimately cell death, even with the downregulated evidence (Allison 2017, Hondorp and Matthews 2004, Yan et al. 2003).

On a whole, EL1-infected *Cassiopea* expressed more DEG than its KB8 heat tolerant counter-part (Figure 4 vs Figure 5). Historically, heat-intolerant species tend to express more genes during times of stress (Bay and Palumbi 2017, DeSalvo et al. 2008). A 2010 study found that corals infected with different symbionts expressed similar genes based on the *Symbiodinium* genotype more than in the same environmental condition (DeSalvo et al. 2010). In the case of EL1-infected *Cassiopea*, the heat intolerant symbiont is extending its physiological properties onto the host organism. In order to prevent further stress, the host might expel the source of the problem, its *Symbiodinium* species. This would explain why EL1-infected corals tend to bleach easier at higher temperatures. KB8-infected *Cassiopea* were also affected by its symbiont group, as it uses the heat-tolerant properties of the *Symbiodinium* to adapt to the higher temperature. Since the *Symbiodinium* were

still benefitting the host instead of damaging it, *Cassiopea* infected with KB8 maintained its symbiotic relationship.

EnrichKEGG data follow the pattern described above, with large amounts of KEGG pathways upregulated on the onset of heat stress, followed by a sharp decrease in pathways with prolonged heat stress, and very little upregulation observed in the comparison of short vs long term heat stress. Among the upregulated genes observed in the control vs 12hrs32° study, protein processing in the ER, lysosome activity, sphingolipid activity, regulation of the actin skeleton, and endocyte activity offer a more extreme hypothesis for cellular activity during these stages. The actin cytoskeleton has been shown to reorganize when exposed to environmental heat stress, acting to combat the negative effective of thermal stress (Fan et al. 2016). Additional stress resistance could be given by chaperone molecules in the ER, which is why protein processing in the ER is upregulated. However, the EL1-infected *Cassiopea* were not able to keep up with the heat stress, as seen in the upregulation of Sphingolipids, lysosomes, and endocytes. Sphingolipids and endocytes have been linked in previous heat stress research, mainly in that cells lacking sphingolipids cannot perform stress induced endocytosis (Bultynck et al. 2006). Lysosome activity has been well documented as well and has been found to induce apoptosis in heat damaged cells (Yi et al. 2017). The control vs long term heat stress data contain two protein pathways (Protein processing in the ER, and protein digestion and absorption), indicating a significant amount of cellular processes localized in the ER. The disappearance of apoptotic pathways and the continuation of DNA repair pathways could either indicate a return to homeostasis, or unregulated cell growth without scheduled death. The second option is more probable given the information in Table 6B, upregulation of oxidative-stress genes in addition to chaperone and damage-repair genes. Instead of disposing the ROS as waste in apoptosis, EL1-infected *Cassiopea* cells

accumulate the toxic cellular product, inducing oxidative stress. A recent study found similar results; corals infected with heat-intolerant *Symbiodinium* spp. expressed high amounts of reactive oxygen species leakage (oxidative stress) after 13 days of heat stress, while the thermo-tolerant infected corals showed no signs of physiological stress (Levin et al. 2016). An upregulation of ROS scavenging and molecular chaperone genes was increased in thermos-tolerant population, decreasing its susceptibility to cellular and physiological damage (Levin et al. 2016).

CONCLUSION:

In conclusion, the infection of *Cassiopea xamachana* by heat intolerant *Symbiodinium* (EL1) did signal different cellular and mechanistic pathways than those signaled by heat tolerant *Symbiodinium* (KB8) in a cnidarian host context. Differential expression of oxidative-stress mediators (downregulation of collagen, upregulation of heat stress proteins) suggests a high attempt by the organism to use its properties for defense, including those attributed to the infected symbiont. Upregulation of ER stress and apoptosis genes between 12 and 36 hours of thermal stress suggests an attempt by the host organism to retain homeostasis by mediating protein refolding and natural cell death. KB8-infected *Cassiopea* proved their resilience to heat stress in the levels of DEGs: very few were expressed in both control v heat stress groups (12 or 36 hours at 32 °). The longer incubation in heat did stress the samples out, as evident in the upregulation of ER stress and apoptosis. However, ER stress genes were downregulated too, suggesting a balance between cell death and healing. Additional evidence for heat tolerance in KB8-infected *Cassiopea* can be seen with the high down-regulation of genes between 12 and 36 hours in thermal stress. ER and Heat stress genes showed decreased activity, suggesting a return to homeostasis and normal activity.

This data now gives future researchers a basis for understanding how symbiont type might influence its hosts performance in thermal stress. The proteins mentioned in this analysis, along with those annotated in the Appendix, can be used in functional genomic studies to test the importance of the proteins. Manipulating a combination of these genes will give scientists a more detailed look at how the host and symbiont interact to create the holobiont response. Once functional assays are performed on the genes, broader inferences can be made regarding the health of *Cassiopea* infected with different *Symbiodinium.*

Ultimately, this paper attempted to provide transcriptomic evidence for the transitive properties of *Symbiodinium* in a host context. As this field of research progresses, scientists will be able to answer how some cnidarians are less susceptible to the negative effects of rising oceanic temperatures. The result will be a more informed idea on symbiotic relationship performance during heat stress, and therefore a more descriptive analysis of how to prevent widespread loss of biodiversity in oceanic systems as the ocean gets warmer.

Appendix A:

DESeq II gene annotations

Table 2A

Domain Name	log2FoldChange	padj	Annotations
TRINITY_DN557656_c_g1_i1	-2.47675	0.91347	
TRINITY_DN254461_c1_g1_i3	-2.11159	0.164344	
TRINITY_DN24892_c_g1_i3	-2.17373	2.75E-09	Glycine-rich RNA-binding protein 2
TRINITY_DN24892_c_g1_i8	-2.14676	0.254773	
TRINITY_DN24892_c_g1_i6	-2.67645	3.49E-08	
TRINITY_DN24892_c_g1_i1	-2.51238	2.75E-09	
TRINITY_DN243613_c3_g1_i2	-1.86139	0.247229	Endo-1,4-beta-xylanase A (Xylanase A) (EC 3.2.1.8) (1,4-beta-D-xylan xylanohydrolase A)
TRINITY_DN254461_c1_g1_i13	-1.83187	0.362646	Serine/arginine-rich splicing factor 4 (Splicing factor, arginine/serine-rich 4)
TRINITY_DN21423_c_g1_i2	-1.7864	0.455226	
TRINITY_DN24892_c_g1_i4	-1.73298	2.75E-09	31 kDa ribonucleoprotein, chloroplastic (CP-RBP31)
TRINITY_DN24892_c_g1_i5	-1.69877	1.24E-08	
TRINITY_DN24892_c_g1_i7	-1.63473	3.68E-08	
TRINITY_DN228153_c2_g1_i4	-1.61962	0.198994	
TRINITY_DN228153_c2_g1_i6	-1.59853	0.239133	
TRINITY_DN264863_c2_g1_i1	-1.54559	0.91347	
TRINITY_DN228153_c2_g1_i7	-1.41698	0.422244	
TRINITY_DN21423_c_g1_i8	-1.37269	0.238146	High mobility group B protein 2 (High mobility group protein B 1) (AtHMGbeta1) (HMG beta 1) (Nucleosome/chromatin assembly factor group D 2) (Nucleosome/chromatin assembly factor group D 2)
TRINITY_DN264259_c3_g3_i3	-1.33631	0.339583	
TRINITY_DN25385_c7_g1_i8	-1.31944	0.419825	

Table 2B

Domain Name	log2FoldChange	padj	Annotation
TRINITY_DN249940_c5_g1_i5	4.320707	0.028643	Coagulation factor IX (EC 3.4.21.22) (Christmas factor) (Plasma thromboplastin component) (PTC) [Cleaved into: Coagulation factor IXa light chain; Coagulation factor IXa heavy chain]
TRINITY_DN265288_c0_g3_i10	4.256319	0.019899	
TRINITY_DN256920_c5_g1_i7	4.080173	0.000455	RNA-binding protein Nova-1 (Neuro-oncological ventral antigen 1) (Ventral neuron-specific protein 1)
TRINITY_DN255665_c0_g1_i1	3.922669	0.048752	
TRINITY_DN246215_c2_g2_i4	3.906324	0.036486	
TRINITY_DN249940_c5_g1_i2	3.813931	0.036486	
TRINITY_DN101045_c0_g1_i2	3.508867	0.02924	
TRINITY_DN249940_c5_g1_i4	3.503417	0.048752	
TRINITY_DN256920_c5_g1_i8	3.405236	0.000334	Peroxisomal targeting signal 2 receptor (PTS2 receptor) (Peroxin-7)
TRINITY_DN249940_c5_g1_i13	3.31804	0.040198	Coagulation factor IX (EC 3.4.21.22) (Christmas factor) [Cleaved into: Coagulation factor IXa light chain; Coagulation factor IXa heavy chain]
TRINITY_DN265288_c0_g3_i4	3.264208	0.042224	
TRINITY_DN249940_c5_g1_i10	3.202271	0.048752	
TRINITY_DN245889_c6_g1_i9	3.100804	0.048752	
TRINITY_DN245889_c6_g1_i8	3.020701	0.016301	
TRINITY_DN259114_c4_g1_i1	3.0129	0.016301	
TRINITY_DN267218_c14_g1_i7	2.584578	0.007964	
TRINITY_DN267111_c1_g1_i1	2.509245	0.009215	
TRINITY_DN245144_c4_g1_i2	2.426086	0.02924	
TRINITY_DN267218_c14_g1_i2	2.366932	0.011984	
TRINITY_DN257313_c6_g1_i2	2.242573	0.031515	
TRINITY_DN267218_c14_g1_i3	2.187992	3.31E-12	
TRINITY_DN225886_c0_g1_i1	2.156017	0.000255	Heat shock protein 83 (HSP 82) (Fragment)
TRINITY_DN265607_c2_g2_i2	2.111871	0.040198	

TRINITY_DN261132_c5_g8_i2	2.083165	0.000913	
TRINITY_DN254582_c0_g1_i9	1.874544	0.000913	
TRINITY_DN260996_c1_g1_i6	1.81916	0.001978	
TRINITY_DN265541_c3_g1_i2	1.747646	0.020261	U1 small nuclear ribonucleoprotein 70 kDa (U1 snRNP 70 kDa) (U1-70K) (snRNP70)
TRINITY_DN225886_c0_g1_i5	1.704263	0.031515	
TRINITY_DN251816_c5_g2_i1	1.5732	0.042224	
TRINITY_DN257676_c0_g1_i4	1.56611	0.020261	Body wall muscle protein HR-29
TRINITY_DN240928_c4_g6_i1	1.409948	0.049525	
TRINITY_DN265959_c4_g2_i3	0.982987	0.021639	
TRINITY_DN265959_c4_g3_i2	0.942658	0.019562	
TRINITY_DN265959_c4_g3_i1	0.931574	0.042224	

TABLE 2: Annotations for Control vs Short Term Heat Stress DEG Results in KB8 infected *Cassiopea*. Pairwise analysis ($p<0.05$) was performed on samples with normal temperatures and an elevated temperature (34 C) for a period of 12 hours in infected *Cassiopea*. Genes were sorted based on decreasing magnitudes of log2FoldChanges. **A.** Down-regulated genes and their differential expression values. **B.** Up-regulated genes and their differential values.

Table 3A

Domain Name	log2FoldChange	padj	Annotation
TRINITY_DN22495_c1_g1_i3	-4.213719	0.1134767	
TRINITY_DN22495_c2_g1_i3	-3.699659	0.1375322	Peroxinectin A (EC 1.11.1.7)
TRINITY_DN26546_c9_g3_i1	-3.6938	0.1593673	
TRINITY_DN22495_c2_g1_i2	-3.656997	0.1693155	
TRINITY_DN26546_c9_g2_i4	-3.645553	0.3163668	Dual oxidase 1 (EC 1.11.1.-) (EC 1.6.3.1)
TRINITY_DN262518_c4_g1_i6	-3.595566	6.25E-09	
TRINITY_DN267419_c9_g1_i12	-3.578353	0.9312728	
TRINITY_DN26546_c9_g2_i2	-3.569164	0.2372746	Follistatin-related protein 4 (Follistatin-like protein 4) (m-D/Bsp12I 1-1)
TRINITY_DN243845_c_g3_i3	-3.552616	0.3261784	

TRINITY_DN257934_c1_g1_i7	-3.35348	0.2717397	
TRINITY_DN262518_c4_g1_i4	-3.311172	0.9686454	
TRINITY_DN255933_c2_g2_i11	-3.287284	0.3739155	
TRINITY_DN262518_c4_g1_i9	-3.166243	4.42E-06	
TRINITY_DN239945_c_g1_i9	-3.138387	0.7232592	
TRINITY_DN255933_c2_g2_i1	-3.181658	0.1766366	
TRINITY_DN262518_c4_g1_i2	-3.259859	0.1594673	
TRINITY_DN239793_c1_g2_i6	-2.998386	0.1643659	
TRINITY_DN26546_c9_g2_i6	-2.961374	0.37527	Eosinophil peroxidase (EPO) (EC 1.11.1.7) [Cleaved into: Eosinophil peroxidase light chain; Eosinophil peroxidase heavy chain]
TRINITY_DN157737_c1_g1_i2	-2.865564	2.28E-06	
TRINITY_DN263552_c5_g2_i9	-2.853276	0.3617552	
TRINITY_DN23547_c2_g1_i4	-2.755969	0.4299883	
TRINITY_DN262518_c4_g1_i5	-2.687838	0.173538	
TRINITY_DN23547_c2_g1_i3	-2.671632	0.7729577	Proline-rich transmembrane protein 1 (Dispanin subfamily D member 1) (DSPD1) (Synapse differentiation-induced protein 4)
TRINITY_DN137123_c_g1_i1	-2.629568	1.90E-06	
TRINITY_DN24757_c_g1_i5	-2.595236	0.1763885	
TRINITY_DN24892_c_g1_i3	-2.575874	5.87E-15	Glycine-rich RNA-binding protein 2
TRINITY_DN24892_c_g1_i6	-2.555282	1.15E-13	
TRINITY_DN23547_c2_g1_i2	-2.543869	0.8277144	Transcription factor MafA (V-maf musculoaponeurotic fibrosarcoma oncogene homolog A)
TRINITY_DN24892_c_g1_i1	-2.512272	5.87E-15	
TRINITY_DN24892_c_g1_i8	-2.499798	3.31E-07	
TRINITY_DN26198_c3_g1_i3	-2.483626	0.1336845	
TRINITY_DN263552_c5_g2_i6	-2.477914	0.1511966	
TRINITY_DN262518_c4_g1_i7	-2.477626	0.2674268	
TRINITY_DN267171_c1_g1_i1	-2.438422	0.2552369	
TRINITY_DN23871_c1_g1_i4	-2.413594	0.5746123	

TRINITY_DN263552_c5_g2_i4	-2.462239	0.1511966	
TRINITY_DN157737_c1_g1_i1	-2.388454	0.7729577	
TRINITY_DN265991_c5_g2_i4	-2.379388	0.4637633	Heat shock protein 83 (HSP 82) (Fragment)
TRINITY_DN261614_c1_g2_i2	-2.316516	0.9312728	
TRINITY_DN266559_c2_g4_i1	-2.282955	0.3261784	Endothelin-converting enzyme homolog (ECE) (EC 3.4.24.-)
TRINITY_DN25464_c2_g4_i3	-2.255158	0.2614234	Peptidyl-prolyl cis-trans isomerase 5 (PPIase 5) (EC 5.2.1.8) (Cyclophilin-5) (Rotamase 5)
TRINITY_DN258276_c2_g2_i6	-2.221987	0.5352763	
TRINITY_DN258276_c2_g2_i3	-2.255849	0.1311554	
TRINITY_DN263552_c5_g2_i5	-2.166347	0.37527	
TRINITY_DN266559_c1_g1_i3	-2.158682	0.2243295	
TRINITY_DN25152_c1_g1_i1	-2.156399	0.2678611	
TRINITY_DN264129_c3_g1_i5	-2.138875	0.7874866	
TRINITY_DN26619_c9_g3_i3	-2.116613	0.216612	Pancreatic secretory granule membrane major glycoprotein GP2 (Pancreatic zymogen granule membrane protein GP-2)
TRINITY_DN264129_c3_g1_i12	-2.933946	0.5352763	
TRINITY_DN23197_c_g1_i8	-2.769812	0.5839159	
TRINITY_DN26619_c8_g1_i1	-2.718646	0.5746123	
TRINITY_DN262114_c2_g1_i1	-2.642482	0.3674149	
TRINITY_DN266559_c1_g1_i5	-2.444428	0.9312728	Membrane metallo-endopeptidase-like 1 (EC 3.4.24.11) (NEP2(m)) (Neprilysin II) (NEPII) (Neprilysin-2) (NEP2) (NL2) [Cleaved into: Membrane metallo-endopeptidase-like 1, soluble form (Neprilysin-2 secreted) (NEP2(s))]
TRINITY_DN264129_c3_g1_i9	-2.344375	0.1763885	
TRINITY_DN25957_c_g1_i22	-2.463756	0.3536697	
TRINITY_DN24892_c_g1_i4	-1.987597	1.15E-13	31 kDa ribonucleoprotein, chloroplastic (CP-RBP31)
TRINITY_DN252699_c5_g1_i5	-1.965245	0.37527	
TRINITY_DN241798_c2_g1_i4	-1.956611	0.7729577	
TRINITY_DN267919_c141_g4_i6	-1.936186	0.6155882	

TRINITY_DN24892_c_g1_i5	-1.891552	1.14E-11	
TRINITY_DN264129_c3_g1_i1	-1.862783	0.4499388	
TRINITY_DN267171_c1_g1_i6	-1.845135	0.4751274	Fibrinogen-like protein A (FREP-A)
TRINITY_DN267171_c1_g1_i9	-1.831649	0.3739155	
TRINITY_DN243613_c3_g1_i2	-1.759387	0.2614234	
TRINITY_DN24892_c_g1_i7	-1.737183	8.53E-01	
TRINITY_DN266559_c2_g1_i6	-1.736326	0.216612	
TRINITY_DN254137_c3_g3_i13	-1.735753	0.2273398	
TRINITY_DN267919_c141_g4_i2	-1.729969	0.3849985	
TRINITY_DN267919_c141_g4_i1	-1.697585	0.4751274	
TRINITY_DN264129_c3_g1_i2	-1.688998	0.2717397	Translocon-associated protein subunit gamma (TRAP-gamma) (Signal sequence receptor subunit gamma) (SSR-gamma)
TRINITY_DN254841_c2_g4_i4	-1.675631	0.328962	Glutamine synthetase 2 cytoplasmic (EC 6.3.1.2) (Glutamate--ammonia ligase 2)
TRINITY_DN26711_c3_g1_i4	-1.668329	0.4767954	
TRINITY_DN263963_c_g1_i14	-1.591839	0.3261784	
TRINITY_DN217288_c_g1_i5	-1.589137	0.4312149	
TRINITY_DN263554_c5_g2_i3	-1.567617	0.4913962	
TRINITY_DN21423_c_g1_i2	-1.537569	0.3269562	
TRINITY_DN264863_c2_g1_i1	-1.538633	0.5785975	
TRINITY_DN25621_c1_g1_i5	-1.477692	0.7558615	Insulin-induced gene 2 protein (INSIG-2)
TRINITY_DN267679_c9_g1_i6	-1.468845	0.3163668	
TRINITY_DN25621_c1_g1_i7	-1.443533	0.1494497	Insulin-induced gene 2 protein (INSIG-2)
TRINITY_DN25621_c1_g1_i2	-1.425423	0.1244242	Ferritin, heavy subunit (Ferritin H) (EC 1.16.3.1)
TRINITY_DN21423_c_g1_i3	-1.394527	0.4115228	High mobility group B protein 2 (High mobility group protein B 1) (AtHMGbeta1) (HMG beta 1) (Nucleosome/chromatin assembly factor group D 2) (Nucleosome/chromatin assembly factor group D 2)
TRINITY_DN21423_c_g1_i6	-1.398534	0.1511966	
TRINITY_DN254841_c2_g4_i2	-1.36245	0.4751274	

TRINITY_DN21423_c_g1_i8	-1.346497	0.9312728	High mobility group-T protein (HMG-T) (HMG-T1) (HMG-1)
TRINITY_DN24292_c1_g2_i1	-1.331164	0.3261784	Protein disulfide-isomerase A5 (EC 5.3.4.1)
TRINITY_DN262622_c2_g1_i9	-1.343636	0.3536697	Collagen alpha-1(XXII) chain
TRINITY_DN229748_c3_g4_i1	-1.31896	0.3536697	
TRINITY_DN26546_c_g1_i6	-1.299877	0.349636	Proline-rich transmembrane protein 1 (Dispanin subfamily D member 1) (DSPD1)
TRINITY_DN193785_c_g1_i4	-1.282844	0.1494497	
TRINITY_DN217288_c_g1_i4	-1.256658	0.1511966	
TRINITY_DN193785_c_g1_i5	-1.252757	0.1164973	
TRINITY_DN26546_c_g1_i8	-1.248192	0.4751274	5'-3' exoribonuclease 3 (AtXRN3) (EC 3.1.13.-) (Protein EXORIBONUCLEASE 3)
TRINITY_DN225114_c4_g1_i4	-1.244875	0.37527	
TRINITY_DN29638_c_g1_i2	-1.155811	0.4115228	Translocon-associated protein subunit gamma (TRAP-gamma) (Signal sequence receptor subunit gamma) (SSR-gamma)
TRINITY_DN23138_c_g2_i1	-1.144342	0.3843826	
TRINITY_DN26532_c6_g1_i4	-1.116492	0.9685829	
TRINITY_DN25445_c8_g3_i1	-1.996218	0.1962141	
TRINITY_DN29638_c_g2_i1	-1.95242	0.4115228	

Table 3B

Domain Name	log2FoldChange	padj	Annotations
TRINITY_DN101045_c0_g1_i2	3.3779382	0.014945	
TRINITY_DN245889_c6_g1_i8	3.1084002	0.0025205	
TRINITY_DN245889_c6_g1_i10	2.8703927	0.0411523	
TRINITY_DN261132_c5_g8_i2	2.7538919	1.45E-08	
TRINITY_DN262009_c0_g1_i1	2.6299618	0.0320618	
TRINITY_DN251816_c5_g2_i1	2.5727145	1.19E-08	

TRINITY_DN261132_c5_g8_i1	2.5409646	3.44E-06	
TRINITY_DN245889_c6_g1_i4	2.455666	0.0116497	
TRINITY_DN267218_c14_g1_i3	2.1348152	2.40E-12	
TRINITY_DN250135_c0_g1_i11	2.1089954	0.0475127	
TRINITY_DN225886_c0_g1_i1	2.0105939	0.000472	
TRINITY_DN230456_c0_g1_i1	1.9120146	0.0411523	Uromodulin (Tamm-Horsfall urinary glycoprotein) (THP) [Cleaved into: Uromodulin, secreted form]
TRINITY_DN260996_c1_g1_i6	1.9046012	0.0002468	Peroxidasin homolog (EC 1.11.1.7)
TRINITY_DN265779_c3_g1_i12	1.8800935	0.0093103	
TRINITY_DN252736_c0_g1_i2	1.7889347	0.035367	
TRINITY_DN248251_c10_g1_i1	1.7512355	0.0498148	
TRINITY_DN254582_c0_g1_i9	1.7148407	0.002127	
TRINITY_DN249243_c10_g7_i1	1.6735183	0.0447553	
TRINITY_DN243347_c3_g3_i2	1.6479601	0.0180321	
TRINITY_DN254437_c4_g1_i4	1.6065364	0.0093103	
TRINITY_DN265541_c3_g1_i2	1.5422473	0.0353058	
TRINITY_DN267026_c3_g3_i1	1.4796949	0.0078075	
TRINITY_DN266937_c5_g2_i2	1.4702514	0.0093103	Fucolectin-4
TRINITY_DN257676_c0_g1_i4	1.3883763	0.0320618	
TRINITY_DN240928_c4_g6_i1	1.3791957	0.0233383	
TRINITY_DN262772_c8_g1_i11	1.1762908	0.0223419	NADPH-dependent aldo-keto reductase, chloroplastic (AtChlAKR) (EC 1.1.1.-) (Aldo-keto reductase family 4 member C9)
TRINITY_DN265959_c4_g2_i3	1.1389878	0.0004314	Heat shock protein HSP 90-alpha
TRINITY_DN265959_c4_g3_i2	1.0469162	0.0007363	
TRINITY_DN265959_c4_g3_i1	1.0195802	0.0035386	Solute carrier family 35 member B1
TRINITY_DN265959_c4_g3_i3	0.9556346	0.0022004	
TRINITY_DN245502_c4_g1_i4	0.8980797	0.0157929	

TABLE 3: Annotations for Control vs Long Term Heat Stress DEG Results in KB8-infected *Cassiopea*.
Pairwise analysis ($p<0.05$) was performed between samples with control temperatures (26° C) incubated for 12 hours and an elevated temperature (34° C) incubated for 36 hours in EL1 infected *Cassiopea*. Genes were sorted based on decreasing magnitudes of log2FoldChanges. **A.** Down-regulated genes and their differential expression values. **B.** Up-regulated genes and their differential expression values.

Table 4A

Domain Name	log2FoldChange	padj	Annotation
TRINITY_DN256724_c_g1_i3	-4.267391667	0.1761874	
TRINITY_DN262518_c4_g1_i4	-4.133992851	3.47E-06	
TRINITY_DN262518_c4_g1_i6	-3.982147799	8.58E-11	
TRINITY_DN256724_c_g1_i4	-3.911824764	0.3515138	Heat shock 7 kDa protein 1-like (Heat shock 7 kDa protein 1L) (Heat shock 7 kDa protein 3) (HSP7.3)
TRINITY_DN262518_c4_g1_i9	-3.858356154	2.22E-09	
TRINITY_DN256724_c_g1_i2	-3.673436317	0.3636639	
TRINITY_DN262518_c4_g1_i2	-3.513886481	2.53E-06	
TRINITY_DN262518_c4_g1_i5	-3.364934349	0.7742417	
TRINITY_DN252532_c7_g1_i4	-2.637528688	0.3852495	Peptidyl-prolyl cis-trans isomerase 5 (PPIase 5) (EC 5.2.1.8) (Cyclophilin-5) (Rotamase 5)
TRINITY_DN26619_c8_g1_i1	-2.423952657	0.6259489	Solute carrier family 35 member B1
TRINITY_DN255933_c2_g2_i1	-2.413269298	0.1895962	
TRINITY_DN23547_c2_g1_i4	-2.386237352	0.7593524	
TRINITY_DN26619_c9_g2_i1	-2.341433429	0.1435368	Pancreatic secretory granule membrane major glycoprotein GP2 (Pancreatic zymogen granule membrane protein GP-2)
TRINITY_DN24757_c_g1_i5	-2.332122485	0.3636639	
TRINITY_DN267171_c1_g1_i1	-2.3716155	0.4272623	
TRINITY_DN26619_c9_g3_i4	-2.214879834	0.3925516	Oncoprotein-induced transcript 3 protein (Liver-specific zona pellucida domain-containing protein)
TRINITY_DN247143_c2_g1_i6	-2.149987293	0.2368844	
TRINITY_DN23547_c2_g1_i3	-2.147812319	0.2711117	Proline-rich transmembrane protein 1 (Dispanin subfamily D member 1) (DSPD1) (Synapse differentiation-induced protein 4)
TRINITY_DN23547_c2_g1_i2	-2.113271213	0.193958	Zona pellucida-like domain-containing protein 1 (ZP domain-containing protein 1) (Cupulin) [Cleaved into: Zona pellucida-like domain-containing protein 1, secreted form]

TRINITY_DN26619_c9_g3_i3	-2.876447448	0.2368844	
TRINITY_DN233534_c7_g1_i1	-1.958693526	0.3852495	Proline-rich transmembrane protein 1 (Dispanin subfamily D member 1) (DSPD1)
TRINITY_DN26642_c4_g3_i2	-1.931736849	0.2675268	Endoplasmin (Heat shock 18 kDa protein) (HSP 18) (HSP18) (Heat shock protein 9 kDa beta member 1) (Transferrin-binding protein)
TRINITY_DN261614_c1_g2_i6	-1.889494947	0.4476872	
TRINITY_DN267914_c22_g2_i1	-1.877482244	0.3424236	
TRINITY_DN26642_c4_g3_i1	-1.866562967	0.3925516	Endoplasmin (94 kDa glucose-regulated protein) (GRP-94) (Heat shock protein 9 kDa beta member 1)
TRINITY_DN26619_c9_g3_i7	-1.864293879	0.1518591	
TRINITY_DN23197_c_g1_i8	-1.794844311	0.3159812	
TRINITY_DN26642_c4_g1_i4	-1.792938163	0.3911754	
TRINITY_DN251417_c5_g1_i1	-1.779169287	0.7426342	
TRINITY_DN264747_c3_g2_i21	-1.757986368	0.3636639	
TRINITY_DN26642_c4_g1_i5	-1.746233385	0.5113188	Endoplasmin (94 kDa glucose-regulated protein) (GRP-94) (98 kDa protein kinase) (PPK 98) (ppk98) (Heat shock protein 9 kDa beta member 1) (gp96 homolog)
TRINITY_DN2613_c1_g1_i2	-1.737269895	0.3925516	Endoplasmic reticulum chaperone BiP (EC 3.6.4.1) (78 kDa glucose-regulated protein) (GRP-78) (Binding-immunoglobulin protein) (BiP) (Heat shock protein 7 family protein 5) (HSP7 family protein 5) (Heat shock protein family A member 5) (Immunoglobulin heavy chain-binding protein)
TRINITY_DN267919_c141_g4_i6	-1.729689683	0.2711117	
TRINITY_DN263554_c5_g2_i3	-1.716764582	0.1945692	
TRINITY_DN2613_c1_g1_i1	-1.78867476	0.4641712	
TRINITY_DN26619_c9_g2_i3	-1.698192415	0.3159812	
TRINITY_DN26642_c4_g1_i7	-1.696253953	0.7593524	
TRINITY_DN261131_c3_g2_i2	-1.684548592	0.2675268	
TRINITY_DN251417_c5_g1_i5	-1.68425298	0.1435368	Protein disulfide-isomerase A4 (EC 5.3.4.1) (Endoplasmic reticulum resident protein 7) (ER

			protein 7) (ERp7) (Endoplasmic reticulum resident protein 72) (ER protein 72) (ERp-72) (ERp72)
TRINITY_DN26711_c3_g1_i4	-1.67285173	0.4476872	Fibrinogen-like protein A (FREP-A)
TRINITY_DN261131_c3_g2_i4	-1.672283478	0.7426342	Mesencephalic astrocyte-derived neurotrophic factor (Arginine-rich protein) (Protein ARMET)
TRINITY_DN26642_c4_g1_i3	-1.662822879	0.7426342	Endoplasmin (94 kDa glucose-regulated protein) (GRP-94) (Endoplasmic reticulum resident protein 99) (ERp99) (Heat shock protein 9 kDa beta member 1) (Polymorphic tumor rejection antigen 1) (Tumor rejection antigen gp96)
TRINITY_DN26642_c4_g1_i1	-1.644958741	0.7593524	
TRINITY_DN26642_c4_g1_i2	-1.643322748	0.7426342	
TRINITY_DN261131_c3_g2_i8	-1.631836962	0.2777417	Mesencephalic astrocyte-derived neurotrophic factor homolog (MANF/CDNF-like protein)
TRINITY_DN251417_c5_g1_i2	-1.617853915	0.152155	
TRINITY_DN242374_c_g1_i4	-1.678911838	0.1147192	
TRINITY_DN25575_c2_g1_i3	-1.5894618	0.2786597	
TRINITY_DN259872_c3_g2_i1	-1.562824466	0.5988452	DBH-like monooxygenase protein 1 homolog (EC 1.14.17.-)
TRINITY_DN2613_c1_g3_i1	-1.551292646	0.2267734	
TRINITY_DN251417_c5_g1_i6	-1.523574283	0.3636639	
TRINITY_DN264747_c3_g2_i8	-1.519698922	0.3711821	Hypoxia up-regulated protein 1
TRINITY_DN251417_c5_g1_i7	-1.574991547	0.1234453	
TRINITY_DN242374_c_g1_i3	-1.562951359	0.2711117	
TRINITY_DN264747_c3_g2_i7	-1.533266965	0.3424236	
TRINITY_DN239873_c1_g1_i4	-1.525628637	0.1885332	
TRINITY_DN259872_c3_g2_i18	-1.488156817	0.1124439	
TRINITY_DN259872_c3_g2_i6	-1.482698286	0.7593524	
TRINITY_DN26665_c_g1_i7	-1.482494135	0.1372214	
TRINITY_DN259872_c3_g2_i17	-1.473629556	0.1761874	
TRINITY_DN259872_c3_g2_i7	-1.467133573	0.1842286	
TRINITY_DN245288_c1_g2_i2	-1.457355184	0.4243481	

TRINITY_DN256164_c1_g4_i1	-1.455737689	0.3142615	Protein disulfide-isomerase A6 (EC 5.3.4.1) (Endoplasmic reticulum protein 5) (ER protein 5) (ERp5) (Protein disulfide isomerase P5) (Thioredoxin domain-containing protein 7)
TRINITY_DN25828_c8_g1_i7	-1.438764858	0.2711117	Calcyclin-binding protein (CacyBP)
TRINITY_DN259872_c3_g2_i12	-1.421142383	0.249482	
TRINITY_DN25828_c8_g1_i8	-1.414794367	0.7273619	
TRINITY_DN251417_c5_g1_i9	-1.398527376	0.4834531	Protein disulfide-isomerase A4 (EC 5.3.4.1) (Endoplasmic reticulum resident protein 72) (ER protein 72) (ERp-72) (ERp72)
TRINITY_DN239873_c1_g1_i2	-1.392694382	0.5113188	
TRINITY_DN259872_c3_g2_i3	-1.375663557	0.1842286	Calumenin-B
TRINITY_DN23798_c1_g1_i1	-1.351652184	0.324427	
TRINITY_DN24292_c1_g2_i1	-1.349463777	0.2711117	
TRINITY_DN239873_c1_g1_i1	-1.327488367	0.1761874	
TRINITY_DN262622_c2_g1_i9	-1.324768695	0.2911497	Peptidyl-prolyl cis-trans isomerase B (PPIase B) (EC 5.2.1.8) (Cyclophilin B) (Rotamase B) (S-cyclophilin) (SCYLP)
TRINITY_DN256164_c1_g2_i1	-1.322684842	0.5113188	
TRINITY_DN256164_c1_g2_i3	-1.318311548	0.1916956	Protein disulfide-isomerase A6 (EC 5.3.4.1) (Thioredoxin domain-containing protein 7)
TRINITY_DN26665_c_g1_i2	-1.289721418	0.2711117	
TRINITY_DN239873_c1_g1_i3	-1.288221877	0.2145127	
TRINITY_DN23798_c1_g1_i1	-1.267362524	0.2368844	
TRINITY_DN25828_c8_g1_i1	-1.266167737	0.2841522	Calreticulin (CRP55) (Calregulin) (Endoplasmic reticulum resident protein 6) (ERp6) (HACBP)
TRINITY_DN23798_c1_g1_i3	-1.255536442	0.2777417	
TRINITY_DN23798_c1_g1_i4	-1.236515354	0.3142615	
TRINITY_DN26665_c_g1_i6	-1.233597181	0.1878564	Calreticulin
TRINITY_DN262622_c2_g1_i1	-1.222835545	0.3159812	
TRINITY_DN26665_c_g1_i3	-1.172339585	0.4592992	Calreticulin

Table 4B

Domain Name	log2FoldChange	padj	Annotations
TRINITY_DN232795_c2_g1_i1	1.3426372	0.1868451	Fucolectin-4
TRINITY_DN232795_c2_g1_i2	1.2481416	0.4243481	
TRINITY_DN232795_c2_g1_i4	1.1771973	0.1147192	
TRINITY_DN25577_c6_g2_i3	0.7353787	0.3852495	DnaJ homolog subfamily C member 3 (Endoplasmic reticulum DNA J domain-containing protein 6) (ER-resident protein ERdj6) (ERdj6) (Interferon-induced, double-stranded RNA-activated protein kinase inhibitor) (Protein kinase inhibitor of 58 kDa) (Protein kinase inhibitor p58)

TABLE 4: Top 100 annotations for Short vs Long Term Heat Stress DEG Results. Pairwise analysis ($p<0.05$) was performed on samples with elevated temperatures (34° C) for a period of 12 and 36 hours in KB8 infected *Cassiopea*. Genes were sorted based on decreasing magnitudes of log2FoldChanges. **A.** Down-regulated genes and their differential expression values. **B.** Up-regulated genes and their differential values.

Table 5A

Domain Name	log2FoldChange	padj	Annotation
TRINITY_DN197449_c0_g1_i2	-10.35637	0.0305555	
TRINITY_DN242189_c0_g1_i2	-4.538356	0.039494	Retinoid isomerohydrolase (EC 3.1.1.64) (All-trans-retinyl-palmitate hydrolase) (Meso-zeaxanthin isomerase) (EC 5.3.3.-) (Retinal pigment epithelium-specific 65 kDa protein) (Retinol isomerase)
TRINITY_DN242189_c0_g1_i3	-4.474521	0.0393426	
TRINITY_DN250729_c6_g1_i3	-3.312612	0.008288	Transcription factor Spi-C
TRINITY_DN254461_c1_g1_i1	-3.128813	3.48E-11	Serine/arginine-rich splicing factor 4 (Pre-mRNA-splicing factor SRP75) (SRP001LB) (Splicing factor, arginine/serine-rich 4)
TRINITY_DN208666_c0_g1_i1	-2.90256	0.0078223	Techylectin-5A
TRINITY_DN254461_c1_g1_i2	-2.83137	1.18E-08	Serine-arginine protein 55 (SRP55) (52 kDa bracketing protein) (B52 protein) (Protein enhancer of deformed)
TRINITY_DN265991_c5_g2_i18	-2.773458	0.0159612	
TRINITY_DN265991_c5_g2_i15	-2.740614	0.011783	

TRINITY_DN254461_c1_g1_i4	-2.543104	2.05E-06	
TRINITY_DN267753_c3_g1_i1	-2.540493	0.0253105	
TRINITY_DN250729_c6_g1_i10	-2.537971	0.0286493	
TRINITY_DN254461_c1_g1_i17	-2.46568	0.000113	
TRINITY_DN248242_c0_g1_i7	-2.30099	0.022723	6-deoxyerythronolide-B synthase EryA1, modules 1 and 2 (DEBS 1) (EC 2.3.1.94) (6-deoxyerythronolide B synthase I) (Erythronolide synthase) (ORF C)
TRINITY_DN258890_c1_g1_i5	-2.248526	0.0193754	Tyrosinase (EC 1.14.18.1) (Monophenol monooxygenase)
TRINITY_DN265991_c5_g2_i20	-2.166817	0.0367993	
TRINITY_DN201423_c0_g1_i8	-2.142181	2.09E-06	
TRINITY_DN265991_c5_g2_i12	-2.1065	0.0234613	
TRINITY_DN265991_c5_g2_i1	-2.08277	0.0255509	
TRINITY_DN231308_c0_g2_i2	-2.05877	0.0440726	
TRINITY_DN264863_c2_g1_i1	-2.048097	2.66E-09	
TRINITY_DN264259_c3_g3_i3	-2.046447	6.51E-07	U1 small nuclear ribonucleoprotein 70 kDa (U1 snRNP 70 kDa) (U1-70K) (snRNP70)
TRINITY_DN265991_c5_g1_i2	-2.012485	0.0041806	
TRINITY_DN256372_c5_g2_i6	-1.99055	0.0115924	
TRINITY_DN264028_c1_g2_i5	-1.893655	0.0479463	Probable ribonuclease ZC3H12C (EC 3.1.-.-) (MCP-induced protein 3) (Zinc finger CCCH domain-containing protein 12C)
TRINITY_DN265991_c5_g2_i10	-1.889572	0.0228637	
TRINITY_DN265991_c5_g2_i16	-1.88163	0.0314681	
TRINITY_DN262173_c0_g4_i2	-1.841849	0.0458718	
TRINITY_DN201423_c0_g1_i2	-1.837672	0.000217	High mobility group B protein 2 (High mobility group protein B 1) (AtHMGbeta1) (HMG beta 1) (Nucleosome/chromatin assembly factor group D 02) (Nucleosome/chromatin assembly factor group D 2)
TRINITY_DN266269_c10_g1_i3	-1.831495	0.0071069	
TRINITY_DN256372_c5_g2_i1	-1.819273	0.0184444	Activating transcription factor of chaperone
TRINITY_DN256372_c5_g2_i4	-1.798469	0.0142611	
TRINITY_DN243613_c3_g1_i2	-1.797168	3.28E-05	

TRINITY_DN254550_c3_g1_i2	-1.790039	0.0001309	Coactosin-like protein
TRINITY_DN201423_c0_g1_i6	-1.789918	0.0001307	High mobility group-T protein (HMG-T) (HMG-T1) (HMG-1)
TRINITY_DN263167_c10_g1_i3	-1.784163	0.0028726	
TRINITY_DN256372_c5_g2_i7	-1.745169	0.0298851	
TRINITY_DN254550_c3_g1_i3	-1.700039	0.0031336	Coactosin-like protein
TRINITY_DN263167_c10_g1_i18	-1.658159	0.0193754	
TRINITY_DN201423_c0_g1_i3	-1.636778	0.0024617	
TRINITY_DN226618_c0_g1_i1	-1.568673	1.48E-08	
TRINITY_DN267196_c4_g3_i3	-1.548267	0.0010233	3-ketoacyl-CoA thiolase, mitochondrial (EC 2.3.1.16) (Acetyl-CoA acyltransferase) (Beta-ketothiolase) (Mitochondrial 3-oxoacyl-CoA thiolase) (T1)
TRINITY_DN228153_c2_g1_i6	-1.527305	0.0003721	
TRINITY_DN260814_c0_g1_i3	-1.526938	0.015205	
TRINITY_DN228153_c2_g1_i3	-1.524604	0.0050086	
TRINITY_DN248920_c0_g1_i1	-1.514452	4.99E-05	Glycine-rich RNA-binding protein 2
TRINITY_DN249805_c3_g1_i1	-1.511049	0.0002229	
TRINITY_DN262173_c0_g3_i1	-1.507055	0.0032088	Coactosin-like protein
TRINITY_DN265302_c6_g1_i4	-1.502826	0.0013169	
TRINITY_DN263403_c5_g1_i6	-1.483326	0.0045879	Prostaglandin reductase 1 (PRG-1) (EC 1.3.1.-) (15-oxoprostaglandin 13-reductase) (EC 1.3.1.48) (Dithiolethione-inducible gene 1 protein) (D3T-inducible gene 1 protein) (DIG-1) (NADP-dependent leukotriene B4 12-hydroxydehydrogenase) (EC 1.3.1.74)
TRINITY_DN236890_c1_g1_i6	-1.471669	3.36E-05	
TRINITY_DN248920_c0_g1_i8	-1.424957	0.0021253	
TRINITY_DN267752_c40_g1_i15	-1.415367	0.0498703	Valine--tRNA ligase (EC 6.1.1.9) (Protein G7a) (Valyl-tRNA synthetase) (ValRS)
TRINITY_DN265331_c2_g1_i6	-1.413647	0.0012625	Hormone-sensitive lipase (HSL) (EC 3.1.1.79)
TRINITY_DN239414_c0_g1_i2	-1.411495	0.0437517	
TRINITY_DN228153_c2_g1_i7	-1.403995	0.0005135	RNA-binding protein Nova-1 (Neuro-oncological ventral antigen 1) (Ventral neuron-specific protein 1)

TRINITY_DN260030_c0_g4_i1	-1.403544	0.0024617	
TRINITY_DN267033_c20_g1_i25	-1.397979	0.0121008	
TRINITY_DN248920_c0_g1_i3	-1.39627	0.0005135	31 kDa ribonucleoprotein, chloroplastic (CP-RBP31)
TRINITY_DN251103_c7_g2_i10	-1.395662	0.0059018	
TRINITY_DN265305_c3_g1_i3	-1.394898	0.0007651	Quinone oxidoreductase (EC 1.6.5.5) (NADPH:quinone reductase) (Zeta-crystallin)
TRINITY_DN262726_c12_g1_i3	-1.392484	0.0125654	
TRINITY_DN267033_c20_g1_i23	-1.386789	0.0231446	COMM domain-containing protein 5 (Hypertension-related calcium-regulated gene protein) (HCaRG)
TRINITY_DN236890_c1_g1_i7	-1.385683	1.98E-05	
TRINITY_DN201423_c0_g1_i1	-1.359425	0.0118656	
TRINITY_DN249805_c3_g1_i2	-1.357017	0.0006977	
TRINITY_DN237850_c0_g1_i2	-1.352351	0.0041494	Histone H2A type 1
TRINITY_DN266269_c10_g1_i2	-1.35202	0.0124354	
TRINITY_DN258351_c8_g2_i2	-1.349866	0.0430495	
TRINITY_DN266269_c10_g3_i1	-1.347974	0.033827	Sphingolipid delta(4)-desaturase DES1 (EC 1.14.19.17) (Degenerative spermatocyte homolog 1)
TRINITY_DN259300_c3_g2_i4	-1.346147	0.0430495	Elongation of very long chain fatty acids protein 4 (EC 2.3.1.199) (3-keto acyl-CoA synthase ELOVL4) (ELOVL fatty acid elongase 4) (ELOVL FA elongase 4) (Very long chain 3-ketoacyl-CoA synthase 4) (Very long chain 3-oxoacyl-CoA synthase 4)
TRINITY_DN265305_c3_g1_i8	-1.343319	0.0424066	
TRINITY_DN265044_c2_g1_i12	-1.33663	0.0125493	Ethanolamine-phosphate phospho-lyase (EC 4.2.3.2) (Alanine--glyoxylate aminotransferase 2-like 1)
TRINITY_DN181520_c0_g1_i1	-1.327892	0.0214019	
TRINITY_DN248920_c0_g1_i4	-1.327702	0.0001546	
TRINITY_DN267196_c4_g3_i4	-1.31955	0.0010363	3-ketoacyl-CoA thiolase, mitochondrial (EC 2.3.1.16) (Acetyl-CoA acyltransferase) (Beta-ketothiolase) (Mitochondrial 3-oxoacyl-CoA thiolase)
TRINITY_DN248920_c0_g1_i5	-1.30432	3.24E-05	
TRINITY_DN193785_c0_g1_i4	-1.294326	0.0358295	
TRINITY_DN248920_c0_g1_i6	-1.290284	0.0210461	

TRINITY_DN257605_c2_g2_i2	-1.289435	0.0241006	Adenylosuccinate synthetase (AMPSase) (AdSS) (EC 6.3.4.4) (IMP--aspartate ligase)
TRINITY_DN264982_c9_g2_i1	-1.286714	0.0450729	
TRINITY_DN266269_c10_g3_i2	-1.273606	0.0203428	
TRINITY_DN250220_c4_g1_i6	-1.269626	0.0152909	Hydroxyacid-oxoacid transhydrogenase, mitochondrial (HOT) (EC 1.1.99.24) (Alcohol dehydrogenase iron-containing protein 1) (ADHFe1)
TRINITY_DN248905_c3_g1_i1	-1.264925	0.0019266	Retinal dehydrogenase 1 (RALDH 1) (RalDH1) (EC 1.2.1.-) (EC 1.2.1.36) (ALDH-E1) (ALHDII) (Aldehyde dehydrogenase family 1 member A1) (Aldehyde dehydrogenase, cytosolic)
TRINITY_DN264981_c1_g1_i16	-1.251522	0.0458718	
TRINITY_DN228153_c2_g1_i4	-1.248325	0.0151748	
TRINITY_DN254318_c3_g1_i7	-1.247825	0.0153065	
TRINITY_DN258736_c0_g1_i2	-1.247224	0.022723	
TRINITY_DN248920_c0_g1_i7	-1.246961	0.000113	
TRINITY_DN264227_c7_g1_i5	-1.244671	0.0279213	Epoxide hydrolase 1 (EC 3.3.2.9) (Epoxide hydratase) (Microsomal epoxide hydrolase) (mEH)
TRINITY_DN237183_c1_g1_i1	-1.232766	0.0125654	Bladder cancer-associated protein
TRINITY_DN264981_c1_g1_i3	-1.228667	0.0401732	Probable ATP-dependent RNA helicase ddx6 (EC 3.6.4.13) (DEAD box protein 6)
TRINITY_DN211823_c1_g1_i5	-1.228388	0.0005135	
TRINITY_DN256178_c1_g1_i11	-1.226116	0.0191537	Platelet-activating factor acetylhydrolase IB subunit beta (EC 3.1.1.47) (PAF acetylhydrolase 30 kDa subunit) (PAF-AH 30 kDa subunit) (PAF-AH subunit beta) (PAFAH subunit beta)
TRINITY_DN266176_c6_g1_i14	-1.217382	0.0234613	Nose resistant to fluoxetine protein 6 (Protein nrf-6)
TRINITY_DN249805_c3_g2_i1	-1.214427	0.0472299	Voltage-gated potassium channel (KvAP)
TRINITY_DN262726_c12_g1_i11	-1.21208	0.020102	
TRINITY_DN227940_c0_g2_i3	-1.202036	0.0004411	Peroxiredoxin-5, mitochondrial (EC 1.11.1.15) (Peroxiredoxin V) (Prx-V) (Thioredoxin peroxidase)
TRINITY_DN227940_c0_g3_i1	-1.19295	7.27E-05	
TRINITY_DN254235_c1_g3_i1	-1.179938	0.0234613	

Table 5B

Domain Name	log2FoldChange	padj	Annotation
TRINITY_DN222493_c0_g1_i6	3.2766148	0.0474922	
TRINITY_DN261132_c5_g8_i2	2.880587	1.88E-13	
TRINITY_DN267218_c14_g1_i3	2.6951818	1.21E-05	
TRINITY_DN265196_c1_g3_i1	2.6163926	0.0023567	
TRINITY_DN267913_c24_g3_i4	2.4474992	0.0007651	Sterol 26-hydroxylase, mitochondrial (EC 1.14.15.15) (5-beta-cholestane-3-alpha,7-alpha,12-alpha-triol 27-hydroxylase) (Cytochrome P-450C27/25) (Cytochrome P450 27) (Sterol 27-hydroxylase) (Vitamin D(3) 25-hydroxylase)
TRINITY_DN243705_c2_g3_i9	2.4217524	0.000863	Cytochrome P450 CYP12A2 (EC 1.14.-.-) (CYPXIIA2)
TRINITY_DN267913_c24_g1_i1	2.4161131	2.48E-05	
TRINITY_DN262740_c2_g1_i3	2.3981154	5.43E-06	
TRINITY_DN262009_c0_g1_i1	2.3620201	0.000217	
TRINITY_DN242729_c1_g1_i1	2.35964	0.0060864	Uncharacterized protein CXorf65 homolog
TRINITY_DN242729_c1_g1_i2	2.3202407	0.0325903	
TRINITY_DN248024_c4_g2_i3	2.2913705	0.0003908	Cytochrome P450 11B, mitochondrial (CYPXIB) (Cytochrome P450C11) (P-450(11 beta,aldo)) (Steroid 11-beta-hydroxylase) (EC 1.14.15.4)
TRINITY_DN224332_c0_g1_i2	2.2671927	0.0004411	
TRINITY_DN248734_c1_g1_i1	2.2483782	0.0027597	
TRINITY_DN199613_c2_g1_i1	2.2319835	0.0021253	
TRINITY_DN252548_c2_g1_i12	2.1151389	0.0067984	
TRINITY_DN199095_c0_g1_i1	2.1055452	0.0055895	Probable cytochrome P450 49a1 (EC 1.14.-.-) (CYPXLIXA1)
TRINITY_DN225886_c0_g1_i5	2.0921442	0.0015607	
TRINITY_DN265900_c4_g1_i4	2.0900487	0.0050275	
TRINITY_DN259593_c2_g1_i4	2.0828147	5.43E-06	
TRINITY_DN252548_c2_g1_i8	2.0784972	0.0021253	
TRINITY_DN248024_c4_g2_i6	2.049612	0.0041494	1,25-dihydroxyvitamin D(3) 24-hydroxylase, mitochondrial (24-OHase) (Vitamin D(3) 24-

			hydroxylase) (EC 1.14.15.16) (Cytochrome P450 24A1) (Cytochrome P450-CC24)
TRINITY_DN252548_c2_g1_i10	2.0289062	0.0177881	Activator of 90 kDa heat shock protein ATPase homolog 2
TRINITY_DN267205_c1_g1_i1	2.0274402	0.0006216	
TRINITY_DN262740_c2_g1_i9	2.0255447	0.000307	
TRINITY_DN265900_c4_g1_i2	2.0047873	0.0234613	
TRINITY_DN261132_c5_g8_i1	2.0038959	0.0011152	
TRINITY_DN255039_c7_g2_i8	1.9904899	0.0102659	
TRINITY_DN240081_c5_g1_i20	1.9689745	0.0493575	
TRINITY_DN257291_c6_g5_i1	1.935556	0.000307	E3 ubiquitin-protein ligase dbl4 (EC 2.3.2.27) (DNA-break-localizing protein 4) (Histone E3 ligase 1) (RING-type E3 ubiquitin transferase dbl4)
TRINITY_DN257291_c6_g5_i8	1.9304657	0.0011963	
TRINITY_DN267913_c22_g1_i1	1.9015015	0.0005473	
TRINITY_DN259593_c2_g1_i3	1.8888628	3.30E-05	
TRINITY_DN259593_c2_g1_i5	1.879781	0.0004214	
TRINITY_DN267913_c22_g1_i2	1.8681919	0.0277023	25-hydroxyvitamin D-1 alpha hydroxylase, mitochondrial (EC 1.14.15.18) (25-OHD-1 alpha-hydroxylase) (25-hydroxyvitamin D(3) 1-alpha-hydroxylase) (VD3 1A hydroxylase) (Calcidiol 1-monooxygenase) (Cytochrome P450 subfamily XXVIIB polypeptide 1) (Cytochrome P450C1 alpha) (Cytochrome P450VD1-alpha) (Cytochrome p450 27B1)
TRINITY_DN193514_c0_g1_i1	1.8572634	0.0234613	
TRINITY_DN258858_c0_g1_i1	1.8400248	0.0279213	
TRINITY_DN266896_c5_g1_i1	1.8323676	0.0061601	
TRINITY_DN224332_c0_g1_i1	1.8218405	0.0012033	Peptidyl-prolyl cis-trans isomerase FKBP4 (PPIase FKBP4) (EC 5.2.1.8) (51 kDa FK506-binding protein) (FKBP51) (52 kDa FK506-binding protein) (52 kDa FKBP) (FKBP-52) (59 kDa immunophilin) (p59) (FK506-binding protein 4) (FKBP-4) (FKBP59) (HSP-binding immunophilin) (HBI) (Immunophilin FKBP52) (Rotamase) [Cleaved into: Peptidyl-prolyl cis-trans isomerase FKBP4, N-terminally processed]

TRINITY_DN168102_c0_g1_i1	1.8162849	0.0029303	
TRINITY_DN257291_c6_g5_i4	1.8146374	0.0039101	
TRINITY_DN256634_c6_g1_i15	1.8107126	0.0005564	Heterogeneous nuclear ribonucleoprotein H (hnRNP H) (Ratsg1) [Cleaved into: Heterogeneous nuclear ribonucleoprotein H, N-terminally processed]
TRINITY_DN257291_c6_g5_i11	1.7838802	0.0003307	
TRINITY_DN267913_c24_g3_i6	1.783239	0.0178559	
TRINITY_DN257291_c6_g5_i6	1.7738138	0.0006977	
TRINITY_DN249902_c8_g1_i1	1.7611356	0.0020339	
TRINITY_DN225886_c0_g1_i1	1.7442932	0.0241203	
TRINITY_DN257291_c6_g5_i12	1.7383947	0.0006907	
TRINITY_DN265779_c3_g1_i18	1.7222929	0.0129909	
TRINITY_DN224332_c0_g1_i6	1.7171378	0.0017489	Peptidyl-prolyl cis-trans isomerase FKBP5 (PPIase FKBP5) (EC 5.2.1.8) (51 kDa FK506-binding protein) (51 kDa FKBP) (FKBP-51) (FK506-binding protein 5) (FKBP-5) (Rotamase)
TRINITY_DN244091_c2_g2_i13	1.7152251	0.0161393	
TRINITY_DN253578_c7_g4_i3	1.709437	0.0021205	
TRINITY_DN259593_c2_g1_i1	1.7030821	0.0011188	
TRINITY_DN252123_c4_g2_i2	1.677268	0.0479463	ATPase WRNIP1 (EC 3.6.1.3) (Werner helicase-interacting protein 1)
TRINITY_DN247498_c1_g5_i1	1.6632515	0.0203428	
TRINITY_DN257291_c6_g5_i9	1.6467155	0.0006216	
TRINITY_DN257291_c6_g5_i13	1.6449211	0.000307	
TRINITY_DN265779_c3_g1_i12	1.6403505	0.0188238	
TRINITY_DN254311_c5_g1_i3	1.6324789	0.0129909	
TRINITY_DN252600_c0_g2_i12	1.6181374	0.0007651	
TRINITY_DN262943_c19_g4_i5	1.6179306	0.0006894	
TRINITY_DN262943_c19_g4_i2	1.6046028	0.0063623	MFS-type transporter SLC18B1 (Solute carrier family 18 member B1)
TRINITY_DN257291_c6_g5_i5	1.5852858	0.0021253	
TRINITY_DN262740_c2_g1_i5	1.5850568	0.0491585	

TRINITY_DN255526_c0_g1_i3	1.5831916	0.0115603	
TRINITY_DN254311_c7_g6_i2	1.5447195	0.0049123	
TRINITY_DN255526_c0_g1_i2	1.5443295	0.0321708	
TRINITY_DN267738_c7_g1_i2	1.5431013	0.0014236	
TRINITY_DN254788_c11_g1_i1	1.5383305	0.0013133	
TRINITY_DN245272_c1_g1_i2	1.5335526	0.0129909	
TRINITY_DN258208_c8_g1_i1	1.5327354	0.0034591	Calcyclin-binding protein (CacyBP)
TRINITY_DN257291_c6_g5_i7	1.5174067	0.0331206	
TRINITY_DN262984_c4_g1_i4	1.511715	0.0036767	Retrovirus-related Pol polyprotein from transposon opus [Includes: Protease (EC 3.4.23.-); Reverse transcriptase (EC 2.7.7.49); Endonuclease]
TRINITY_DN262943_c19_g4_i4	1.4910251	0.0048937	MFS-type transporter SLC18B1 (Solute carrier family 18 member B1)
TRINITY_DN255931_c0_g1_i1	1.4789797	4.40E-05	DnaJ homolog subfamily B member 4
TRINITY_DN249902_c8_g1_i2	1.4667677	0.0493575	DnaJ homolog subfamily B member 5 (Heat shock protein Hsp40-3) (Heat shock protein cognate 40) (Hsc40)
TRINITY_DN258208_c8_g1_i7	1.4439779	0.0424535	
TRINITY_DN261876_c1_g1_i9	1.4403063	0.0091611	Heat shock protein 105 kDa (Heat shock 110 kDa protein)
TRINITY_DN199281_c0_g2_i2	1.435427	0.011408	
TRINITY_DN259593_c2_g1_i2	1.4211893	0.0129909	
TRINITY_DN267513_c5_g1_i1	1.4137465	0.0054781	
TRINITY_DN264806_c6_g1_i11	1.3822517	0.0209041	
TRINITY_DN265187_c3_g1_i14	1.378558	0.0222303	
TRINITY_DN267738_c7_g1_i1	1.3595244	0.0241006	
TRINITY_DN258208_c8_g1_i6	1.3326035	0.0301618	Calcyclin-binding protein (CacyBP)
TRINITY_DN199281_c0_g2_i1	1.315366	0.0186856	
TRINITY_DN258155_c3_g2_i9	1.315189	0.0010498	
TRINITY_DN241537_c1_g1_i3	1.3079004	0.0221973	60 kDa heat shock protein, mitochondrial (EC 3.6.4.9) (60 kDa chaperonin) (Chaperonin 60) (CPN60) (Heat shock protein 60) (HSP-60) (Hsp60) (Mitochondrial matrix protein P1)

TRINITY_DN245051_c3_g1_i4	1.3031491	0.042333	Serine/threonine-protein kinase RIO3 (EC 2.7.11.1) (RIO kinase 3)
TRINITY_DN261255_c3_g1_i1	1.2996297	0.0059409	Stress-induced-phosphoprotein 1 (STI1) (Hsc70/Hsp90-organizing protein) (Hop)
TRINITY_DN250904_c11_g1_i6	1.2973825	0.011408	
TRINITY_DN230599_c4_g1_i4	1.2854246	0.0035373	
TRINITY_DN241537_c1_g1_i4	1.2830689	0.0147668	60 kDa heat shock protein, mitochondrial (EC 3.6.4.9) (60 kDa chaperonin) (Chaperonin 60) (CPN60) (Heat shock protein 60) (HSP-60) (Hsp60)
TRINITY_DN261255_c3_g1_i2	1.2786551	0.0284095	Hsp70-Hsp90 organizing protein 2 (AtHop2)
TRINITY_DN259820_c0_g1_i7	1.2706993	0.0450566	
TRINITY_DN249902_c8_g1_i3	1.2682816	0.022723	
TRINITY_DN265880_c5_g1_i7	1.2650631	0.0117282	
TRINITY_DN267289_c3_g1_i3	1.261188	0.0003721	Helicase SKI2W (Ski2) (EC 3.6.4.-) (Helicase-like protein) (HLP)
TRINITY_DN259820_c0_g1_i3	1.2478662	0.0481013	Leukocyte receptor cluster member 9
TRINITY_DN259820_c0_g1_i4	3.2766148 and 1.2293128	0.0485622	

TABLE 5: Top 100 Gene Annotations for Control vs Short Term Heat Stress DEG Results. Pairwise analysis ($p<0.05$) was performed on samples with normal temperatures and an elevated temperature (34° C) for a period of 12 hours in EL1 infected *Cassiopea*. Genes were sorted based on decreasing magnitudes of log2FoldChanges. **A.** Down-regulatedDown-regulated genes and their differential expression values. **B.** Up-regulatedUp-regulated

Tablel 6A

Domain Name	log2FoldChange	padj	Annotation
TRINITY_DN197449_c_g1_i2	-12.48912	0.2515417	
TRINITY_DN476428_c_g1_i1	-6.439629	0.1984235	
TRINITY_DN19989_c2_g2_i3	-6.299549	9.48E-01	
TRINITY_DN19819_c_g2_i1	-3.122775	0.2776634	
TRINITY_DN266843_c2_g2_i17	-2.865112	0.2619326	
TRINITY_DN266843_c2_g2_i15	-2.638783	0.2535947	Collagen-like protein 7
TRINITY_DN266843_c2_g2_i11	-2.498763	0.2656817	

TRINITY_DN266132_c1_g3_i1	-2.455994	0.9962837	
TRINITY_DN254444_c_g1_i3	-2.447624	0.5378954	
TRINITY_DN26714_c6_g2_i2	-2.443263	0.1457934	
TRINITY_DN266257_c3_g1_i18	-2.386885	0.2846327	
TRINITY_DN26714_c6_g1_i13	-2.356828	0.3967814	
TRINITY_DN26714_c6_g2_i1	-2.268318	0.1483753	
TRINITY_DN193514_c_g1_i3	-2.172872	0.425666	Chitotriosidase-1 (EC 3.2.1.14) (Chitinase-1)
TRINITY_DN266843_c2_g2_i1	-2.166977	0.8834941	
TRINITY_DN266132_c1_g3_i4	-2.155318	0.1552989	
TRINITY_DN266132_c1_g3_i3	-1.982869	0.5378954	
TRINITY_DN266132_c1_g3_i5	-1.966944	0.8712528	
TRINITY_DN265286_c5_g2_i16	-1.954227	0.4582933	
TRINITY_DN266132_c1_g3_i2	-1.941825	0.1575776	
TRINITY_DN24892_c_g1_i3	-1.932899	1.88E-01	31 kDa ribonucleoprotein, chloroplastic (CP-RBP31)
TRINITY_DN25113_c7_g2_i15	-1.927746	0.1856395	
TRINITY_DN258218_c4_g1_i3	-1.922894	0.388425	Phenylalanine-4-hydroxylase (PAH) (EC 1.14.16.1) (Phe-4-monooxygenase)
TRINITY_DN266257_c3_g1_i19	-1.915493	0.1684338	
TRINITY_DN265817_c5_g3_i2	-1.899737	0.4112664	Receptor-type tyrosine-protein phosphatase mu (Protein-tyrosine phosphatase mu) (R-PTP-mu) (EC 3.1.3.48)
TRINITY_DN266843_c2_g2_i22	-1.891358	0.3319884	Collagen alpha-1(XXIV) chain
TRINITY_DN21423_c_g1_i8	-1.879768	0.2469244	
TRINITY_DN262395_c3_g1_i17	-1.877275	0.2697718	
TRINITY_DN266132_c1_g1_i3	-1.864813	0.9237545	
TRINITY_DN24892_c_g1_i8	-1.848788	0.13872	
TRINITY_DN251244_c1_g1_i8	-1.846158	0.165698	
TRINITY_DN265143_c2_g1_i9	-1.841974	0.4822958	
TRINITY_DN24892_c_g1_i6	-1.841442	0.6789284	

TRINITY_DN24892_c_g1_i1	-1.834768	2.79E-01	Glycine-rich RNA-binding protein 2
TRINITY_DN26658_c4_g1_i2	-1.827483	0.4771783	Hemicentin-1 (Fibulin-6) (FIBL-6)
TRINITY_DN25513_c1_g1_i11	-1.814343	0.1979874	
TRINITY_DN266132_c1_g1_i17	-1.789437	0.2776634	
TRINITY_DN262395_c3_g1_i9	-1.773682	0.3413849	MAM and LDL-receptor class A domain-containing protein 2 (Skeletal organic matrix MAM and LDL-receptor 2) (SOM MAM and LDL-receptor 2) (Fragment)
TRINITY_DN265143_c2_g1_i2	-1.772985	0.1418989	Highly reducing polyketide synthase azaB (HR-PKS azaB) (EC 2.3.1.-) (Azaphilone biosynthesis cluster protein azaB)
TRINITY_DN258218_c4_g1_i11	-1.769219	0.4537425	
TRINITY_DN24892_c_g1_i7	-1.756732	0.8191584	
TRINITY_DN262893_c2_g1_i4	-1.739125	0.1174538	A disintegrin and metalloproteinase with thrombospondin motifs 9 (ADAM-TS 9) (ADAM-TS9) (ADAMTS-9) (EC 3.4.24.-)
TRINITY_DN262996_c14_g3_i19	-1.733562	0.1866245	
TRINITY_DN247655_c2_g1_i1	-1.731342	0.6791728	von Willebrand factor A domain-containing protein 1
TRINITY_DN265143_c2_g1_i5	-1.723533	0.1888137	
TRINITY_DN178917_c_g1_i1	-1.718634	0.2917576	
TRINITY_DN247655_c5_g2_i4	-1.71162	0.2339386	
TRINITY_DN21423_c_g1_i6	-1.696746	0.1174538	High mobility group-T protein (HMG-T) (HMG-T1) (HMG-1)
TRINITY_DN266549_c6_g1_i3	-1.684592	0.1223186	Low-density lipoprotein receptor-related protein 4 (LRP-4) (LDLR dan)
TRINITY_DN247655_c5_g2_i3	-1.675433	0.1142895	Collagen alpha-6(VI) chain
TRINITY_DN266132_c1_g1_i13	-1.673828	0.8481675	
TRINITY_DN3994_c1_g1_i4	-1.655999	0.2615297	
TRINITY_DN266132_c1_g1_i1	-1.655943	0.2412923	Collagen alpha-2(V) chain
TRINITY_DN21423_c_g1_i2	-1.643553	0.5124843	High mobility group B protein 2 (High mobility group protein B 1)

			(AtHMGbeta1) (HMG beta 1) (Nucleosome/chromatin assembly factor group D 2) (Nucleosome/chromatin assembly factor group D 2)
TRINITY_DN26577_c3_g1_i4	-1.637359	0.1112456	
TRINITY_DN253828_c9_g2_i3	-1.628399	0.2515218	Uncharacterized protein YMR196W
TRINITY_DN267753_c3_g2_i2	-1.618521	0.2315524	Reducing polyketide synthase hmp8 (R-PKS hmp8) (EC 2.3.1.-) (Hypothemycin biosynthesis cluster protein hpm8)
TRINITY_DN266843_c2_g2_i9	-1.614155	0.2166882	
TRINITY_DN266257_c3_g1_i2	-1.597175	0.1988221	Multidrug resistance-associated protein 1 (ATP-binding cassette sub-family C member 1) (Leukotriene C(4) transporter) (LTC4 transporter)
TRINITY_DN266843_c2_g2_i3	-1.589867	0.5994629	
TRINITY_DN262521_c_g1_i6	-1.582522	0.19613	
TRINITY_DN233145_c6_g3_i9	-1.581466	0.4544297	Cartilage matrix protein (Matrilin-1)
TRINITY_DN243613_c3_g1_i2	-1.574377	0.1915398	
TRINITY_DN26658_c4_g1_i7	-1.562863	0.3493932	
TRINITY_DN26445_c4_g2_i7	-1.548685	0.1886172	Solute carrier family 28 member 3 (Concentrative Na(+)-nucleoside cotransporter 3) (hfCNT)
TRINITY_DN26577_c3_g1_i9	-1.54177	0.5972176	Angiotensin-converting enzyme (EC 3.4.15.1) (Dipeptidyl carboxypeptidase I) (Kininase II) (TtACE)
TRINITY_DN26577_c3_g1_i12	-1.538678	0.5972176	
TRINITY_DN233145_c6_g3_i17	-1.536862	0.2461627	
TRINITY_DN267753_c2_g1_i4	-1.526697	6.46E-06	Reducing polyketide synthase PKS1 (EC 2.3.1.-) (T-toxin biosynthesis protein PKS1)
TRINITY_DN266257_c3_g1_i6	-1.519163	0.3955956	
TRINITY_DN26252_c5_g1_i1	-1.489578	0.9758179	Sodium/glucose cotransporter 2 (Na(+)/glucose cotransporter 2) (Low affinity sodium-glucose cotransporter) (Solute carrier family 5 member 2)
TRINITY_DN25513_c1_g1_i9	-1.487934	0.4582823	

TRINITY_DN233145_c6_g3_i11	-1.483639	0.1484492	
TRINITY_DN266257_c3_g1_i14	-1.475586	0.723956	
TRINITY_DN26577_c3_g1_i2	-1.471776	0.2163323	Angiotensin-converting enzyme (ACE) (EC 3.2.1.-) (EC 3.4.15.1) (Dipeptidyl carboxypeptidase I) (Kininase II) (CD antigen CD143) [Cleaved into: Angiotensin-converting enzyme, soluble form]
TRINITY_DN262893_c2_g2_i3	-1.465818	0.3912755	Collagen alpha-5(VI) chain (Collagen alpha-1(XXIX) chain) (von Willebrand factor A domain-containing protein 4)
TRINITY_DN262996_c14_g3_i7	-1.458945	0.2649779	C3 and PZP-like alpha-2-macroglobulin domain-containing protein 8
TRINITY_DN233145_c6_g3_i24	-1.456384	0.2287288	
TRINITY_DN233145_c6_g3_i15	-1.456177	0.1683166	Vitrin
TRINITY_DN265143_c2_g1_i6	-1.447192	0.5211784	
TRINITY_DN266257_c3_g1_i13	-1.442277	0.2776634	Multidrug resistance-associated protein 1 (ATP-binding cassette sub-family C member 1) (Leukotriene C(4) transporter) (LTC4 transporter)
TRINITY_DN25513_c1_g1_i1	-1.441872	0.7413579	Collagen alpha-1(III) chain
TRINITY_DN266257_c3_g1_i7	-1.441181	0.1317612	
TRINITY_DN24892_c_g1_i5	-1.437844	2.69E-01	
TRINITY_DN26718_c2_g4_i27	-1.427954	0.4786941	
TRINITY_DN258926_c5_g3_i5	-1.416377	0.2857888	N-acetylated-alpha-linked acidic dipeptidase 2 (EC 3.4.17.21) (Glutamate carboxypeptidase III) (GCPIII) (N-acetylated-alpha-linked acidic dipeptidase II) (NAALADase II)
TRINITY_DN265143_c2_g1_i1	-1.415964	0.1575776	Reducing polyketide synthase FUB1 (EC 2.3.1.-) (Fusaric acid biosynthesis protein 1)
TRINITY_DN264863_c2_g1_i1	-1.393175	0.5269249	
TRINITY_DN25513_c1_g1_i1	-1.38957	0.2412923	Collagen alpha-1(II) chain (Alpha-1 type II collagen)
TRINITY_DN23689_c1_g1_i6	-1.388579	0.4658494	

TRINITY_DN233145_c6_g3_i13	-1.375773	0.4679418	
TRINITY_DN24892_c_g1_i4	-1.373353	0.4353862	
TRINITY_DN26162_c8_g1_i7	-1.372182	0.2776634	
TRINITY_DN25513_c1_g1_i6	-1.367887	0.1951464	Collagen alpha-1(III) chain (Fragments)
TRINITY_DN266843_c2_g2_i2	-1.36658	0.2159915	Collagen alpha-1(II) chain (Alpha-1 type II collagen)
TRINITY_DN26718_c2_g4_i22	-1.338658	0.1756622	
TRINITY_DN233145_c6_g3_i1	-1.333648	0.1546289	
TRINITY_DN26627_c7_g3_i3	-1.325738	0.9758179	A disintegrin and metalloproteinase with thrombospondin motifs 12 (ADAM-TS 12) (ADAM-TS12) (ADAMTS-12) (EC 3.4.24.-)
TRINITY_DN25513_c1_g1_i7	-1.323385	0.1379381	Collagen alpha-1(I) chain (Alpha-1 type I collagen)

Table 6B

Domain Name	log2FoldChange	padj	Annotation
TRINITY_DN247428_c2_g4_i5	7.5193117	0.2831484	
TRINITY_DN264332_c3_g2_i1	7.1751867	0.1484492	Oxygen-dependent coproporphyrinogen-III oxidase (COX) (Coprogen oxidase) (Coproporphyrinogenase) (EC 1.3.3.3)
TRINITY_DN256724_c_g1_i5	6.9612487	0.1561598	
TRINITY_DN261341_c3_g1_i2	6.3537884	0.3667587	
TRINITY_DN256724_c_g1_i3	6.2762577	0.7915189	Heat shock 7 kDa protein 1-like (Heat shock 7 kDa protein 1L) (Heat shock 7 kDa protein 3) (HSP7.3)
TRINITY_DN49732_c_g1_i1	6.2111944	0.6668121	
TRINITY_DN256724_c_g1_i4	5.4821713	0.9132779	
TRINITY_DN22913_c1_g2_i5	5.4493246	0.133435	
TRINITY_DN254387_c2_g1_i1	5.3358512	0.2467468	
TRINITY_DN261341_c3_g1_i8	5.2739463	0.2163323	

TRINITY_DN222493_c_g1_i6	5.1742925	0.467766	
TRINITY_DN2481_c5_g1_i12	4.9931219	0.3724836	
TRINITY_DN254387_c2_g1_i2	4.8418627	0.5526562	
TRINITY_DN22847_c8_g1_i3	4.8366662	0.3787697	
TRINITY_DN251595_c4_g1_i6	4.6237235	0.2235492	
TRINITY_DN237644_c1_g1_i2	4.5879732	0.1137159	Photosystem I P7 chlorophyll a apoprotein A1 (EC 1.97.1.12) (PSI-A) (PsaA)
TRINITY_DN256724_c_g1_i1	4.5245292	0.6791728	Heat shock cognate 71 kDa protein (Heat shock 7 kDa protein 8)
TRINITY_DN256415_c4_g1_i3	4.4872329	0.2677839	
TRINITY_DN265741_c3_g1_i1	4.4517548	0.3727925	
TRINITY_DN25692_c5_g1_i8	4.4344916	0.3136676	
TRINITY_DN127349_c4_g1_i1	4.4152899	0.1467365	
TRINITY_DN256724_c_g1_i2	4.3992948	0.8973242	
TRINITY_DN251595_c4_g1_i16	4.3141722	0.2792566	
TRINITY_DN263938_c8_g2_i1	4.2632134	0.1828225	
TRINITY_DN25692_c5_g1_i7	4.2626913	0.2535947	Peroxisomal targeting signal 2 receptor (PTS2 receptor) (Peroxin-7)
TRINITY_DN26799_c63_g1_i8	4.2369322	0.1633182	
TRINITY_DN251595_c4_g1_i7	4.2177846	0.2847168	
TRINITY_DN267684_c1_g1_i1	4.1882257	0.3282127	
TRINITY_DN267684_c1_g1_i3	4.1721458	3.76E-01	
TRINITY_DN263938_c8_g4_i1	4.1532425	0.4665342	
TRINITY_DN26799_c63_g1_i3	3.9344876	0.1337982	
TRINITY_DN259481_c3_g1_i16	3.8681163	0.8963553	
TRINITY_DN26726_c5_g4_i2	3.8181292	0.4841439	
TRINITY_DN261132_c5_g8_i2	3.7993423	5.63E-15	
TRINITY_DN215974_c_g1_i1	3.7875373	9.47E-08	Heat shock protein 67B1
TRINITY_DN248855_c1_g4_i1	3.6985448	2.69E-01	
TRINITY_DN24219_c5_g1_i8	3.6839737	0.3589942	
TRINITY_DN263784_c1_g2_i1	3.6368193	0.3698955	

TRINITY_DN2481_c5_g1_i2	3.5972482	1.35E-01	
TRINITY_DN248855_c1_g4_i2	3.58736	0.9158197	
TRINITY_DN224332_c_g1_i4	3.5783935	0.3955956	
TRINITY_DN262755_c3_g1_i2	3.5685621	0.2235492	
TRINITY_DN224332_c_g1_i3	3.3948432	0.1778722	
TRINITY_DN224332_c_g1_i2	3.3938797	1.88E-01	
TRINITY_DN257145_c5_g3_i8	3.3786895	0.2339386	
TRINITY_DN263938_c8_g1_i3	3.3462248	0.8689461	
TRINITY_DN248751_c_g2_i2	3.2147962	0.3226232	Protein windbeutel (Erp29 homolog)
TRINITY_DN244373_c_g1_i1	3.1636732	0.7619938	
TRINITY_DN247189_c_g1_i1	2.9372921	0.418173	Y+L amino acid transporter 2 (Solute carrier family 7 member 6) (y(+)L-type amino acid transporter 2) (Y+LAT2) (y+LAT-2)
TRINITY_DN2526_c_g2_i12	2.9311854	8.27E-06	
TRINITY_DN242247_c5_g1_i1	2.8935438	0.3932847	
TRINITY_DN244989_c_g1_i1	2.7459382	0.1318166	
TRINITY_DN244989_c_g1_i2	2.7139232	0.4526328	
TRINITY_DN224332_c_g1_i5	2.6924125	0.3955956	Peptidyl-prolyl cis-trans isomerase FKBP5 (PPIase FKBP5) (EC 5.2.1.8) (FK56-binding protein 5) (FKBP-5) (Rotamase)
TRINITY_DN258126_c2_g6_i2	2.6612753	0.4582933	
TRINITY_DN267218_c14_g1_i7	2.6593268	0.1317787	
TRINITY_DN254311_c7_g6_i2	2.6582226	0.1112456	
TRINITY_DN254879_c3_g4_i1	2.6455561	0.167925	
TRINITY_DN264684_c1_g2_i3	2.5869775	0.1269176	
TRINITY_DN261132_c5_g8_i1	2.5466321	0.4412356	
TRINITY_DN24817_c7_g1_i4	2.5417686	0.1778722	
TRINITY_DN264788_c5_g1_i12	2.5134335	0.425666	
TRINITY_DN248751_c_g2_i5	2.4999466	0.7588463	Endoplasmic reticulum resident protein 29 (ERp29) (Endoplasmic reticulum resident protein 31) (ERp31)
TRINITY_DN26649_c9_g1_i7	2.4617769	0.2669654	

TRINITY_DN216375_c_g1_i1	2.4464667	0.455353	
TRINITY_DN267141_c3_g1_i12	2.4142692	0.4747779	
TRINITY_DN257283_c3_g2_i17	2.4139743	0.3599937	
TRINITY_DN221661_c_g1_i1	2.4129819	0.1575776	NPC intracellular cholesterol transporter 2 homolog a (Niemann Pick type C2 protein homolog)
TRINITY_DN264684_c1_g2_i2	2.3876173	0.645584	
TRINITY_DN185527_c_g1_i1	2.3865163	0.2615297	
TRINITY_DN252548_c2_g1_i1	2.3825715	0.2329849	Activator of 9 kDa heat shock protein ATPase homolog 1 (AHA1) (p38)
TRINITY_DN265326_c4_g2_i4	2.3739147	0.3912755	
TRINITY_DN261894_c_g3_i2	2.3621686	0.1126442	Poly [ADP-ribose] polymerase 14 (PARP-14) (EC 2.4.2.3) (ADP-ribosyltransferase diphtheria toxin-like 8) (ARTD8) (Collaborator of STAT6) (CoaSt6)
TRINITY_DN267218_c14_g1_i3	2.3161915	0.2252858	
TRINITY_DN224332_c_g1_i1	2.2837883	0.13872	Peptidyl-prolyl cis-trans isomerase FKBP4 (PPIase FKBP4) (EC 5.2.1.8) (51 kDa FK56-binding protein) (FKBP51) (52 kDa FK56-binding protein) (52 kDa FKBP) (FKBP-52) (59 kDa immunophilin) (p59) (FK56-binding protein 4) (FKBP-4) (FKBP59) (HSP-binding immunophilin) (HBI) (Immunophilin FKBP52) (Rotamase) [Cleaved into: Peptidyl-prolyl cis-trans isomerase FKBP4, N-terminally processed]
TRINITY_DN255526_c_g1_i2	2.2826214	0.6146364	
TRINITY_DN2613_c1_g3_i1	2.2559897	0.1764115	
TRINITY_DN26274_c2_g1_i9	2.2473623	0.2163323	
TRINITY_DN2526_c_g2_i3	2.2457332	0.2991735	
TRINITY_DN225886_c_g1_i5	2.2437129	0.244692	
TRINITY_DN23456_c_g1_i1	2.2135587	0.1411519	Transcription factor MafA (V-maf musculoaponeurotic fibrosarcoma oncogene homolog A)
TRINITY_DN255526_c_g1_i3	2.1739764	0.3136676	
TRINITY_DN262454_c2_g1_i1	2.1696466	0.5451682	
TRINITY_DN264788_c5_g1_i8	2.1689322	0.2329849	
TRINITY_DN25828_c8_g1_i6	2.1629862	0.338125	Calcyclin-binding protein (CacyBP)

TRINITY_DN224332_c_g1_i6	1.9939237	0.7527196	Peptidyl-prolyl cis-trans isomerase FKBP5 (PPIase FKBP5) (EC 5.2.1.8) (51 kDa FK56-binding protein) (51 kDa FKBP) (FKBP-51) (FK56-binding protein 5) (FKBP-5) (Rotamase)
TRINITY_DN26274_c2_g1_i4	1.9558747	0.3319884	
TRINITY_DN264788_c5_g1_i3	1.9538318	0.3787697	
TRINITY_DN25828_c8_g1_i7	1.9422612	0.6423876	
TRINITY_DN264788_c5_g1_i1	1.9379317	0.1477199	
TRINITY_DN252441_c7_g1_i3	1.9349624	0.2162674	
TRINITY_DN26642_c4_g3_i2	1.9212721	0.2273219	
TRINITY_DN243654_c1_g1_i2	1.9115479	0.9132779	
TRINITY_DN25828_c8_g1_i8	1.8944768	0.3247543	
TRINITY_DN252548_c2_g1_i8	1.889527	0.4526328	
TRINITY_DN25828_c8_g1_i1	1.8882919	0.4353862	Calcyclin-binding protein (CacyBP)
TRINITY_DN23798_c1_g1_i5	1.8727589	0.1321892	
TRINITY_DN238376_c_g1_i1	1.8668829	0.119214	Calpain-3 (EC 3.4.22.54) (Calcium-activated neutral proteinase 3) (CANP 3) (Calpain L3) (Calpain p94) (Muscle-specific calcium-activated neutral protease 3) (New calpain 1) (nCL-1)
TRINITY_DN255499_c6_g3_i2	1.8597758	0.4582933	
TRINITY_DN26642_c4_g3_i1	1.8592549	0.2415691	Endoplasmin (Heat shock 18 kDa protein) (HSP 18) (HSP18) (Heat shock protein 9 kDa beta member 1) (Transferrin-binding protein)

TABLE 6: Top 100 Gene Annotations for Control vs Short Term Heat Stress DEG Results. Pairwise analysis ($p<0.05$) was performed on samples with normal temperatures and an elevated temperature (34° C) for a period of 12 hours in EL1 infected *Cassiopea*. Genes were sorted based on decreasing magnitudes of log2FoldChanges. **A.** Down-regulatedDown-regulated genes and their differential expression values. **B.** Up-regulatedUp-regulated

Table 7A

Domain Names	log2FoldChange	padj	Annotation
TRINITY_DN265196_c1_g3_i1	-4.144577	2.36E-01	

TRINITY_DN21489_c_g2_i2	-3.864616	0.6316656	
TRINITY_DN248613_c_g1_i5	-3.829218	3.77E-01	
TRINITY_DN219442_c_g1_i2	-3.825489	0.1582461	
TRINITY_DN262938_c_g1_i2	-3.715223	0.1657	
TRINITY_DN192751_c1_g2_i2	-3.675432	0.1288545	
TRINITY_DN262938_c_g1_i1	-3.624154	0.867132	Zinc metalloproteinase nas-4 (EC 3.4.24.-) (Nematode astacin 4)
TRINITY_DN11472_c_g1_i1	-3.595685	0.3157667	
TRINITY_DN257895_c8_g1_i1	-3.574213	0.48325	
TRINITY_DN11573_c_g1_i1	-3.536197	0.1448264	
TRINITY_DN18415_c1_g1_i1	-3.513983	0.8471166	
TRINITY_DN235269_c_g1_i9	-3.488491	0.371297	
TRINITY_DN235269_c_g1_i8	-3.486453	0.649132	Zinc finger RNA-binding protein 2
TRINITY_DN193514_c_g1_i3	-3.482393	1.36E-01	Chitotriosidase-1 (EC 3.2.1.14) (Chitinase-1)
TRINITY_DN223288_c_g1_i1	-3.442282	3.66E-01	
TRINITY_DN34761_c_g1_i1	-3.431696	0.1191962	
TRINITY_DN193514_c_g1_i1	-3.344995	1.50E-01	
TRINITY_DN19819_c_g2_i1	-3.259884	0.23263	
TRINITY_DN28548_c_g2_i5	-3.238246	0.2456974	
TRINITY_DN263826_c1_g1_i22	-3.237742	0.9217371	
TRINITY_DN258396_c1_g1_i9	-3.233796	0.3468217	
TRINITY_DN181959_c1_g1_i4	-3.231397	0.282416	
TRINITY_DN193514_c_g1_i4	-3.196797	6.81E-01	Acidic mammalian chitinase (AMCase) (EC 3.2.1.14)
TRINITY_DN25776_c4_g2_i2	-3.177546	0.399697	
TRINITY_DN214393_c3_g1_i6	-3.127959	1.95E-01	
TRINITY_DN264838_c13_g2_i4	-2.962269	0.787592	
TRINITY_DN21499_c1_g1_i1	-2.946258	0.1875323	Retrovirus-related Pol polyprotein from transposon TNT 1-94 [Includes: Protease (EC 3.4.23.-); Reverse transcriptase (EC 2.7.7.49); Endonuclease]

TRINITY_DN262215_c2_g2_i9	-2.942537	0.2642	
TRINITY_DN267198_c2_g1_i1	-2.936795	0.198388	Coagulation factor VIII (Antihemophilic factor) (AHF) (Procoagulant component) [Cleaved into: Factor VIIIa heavy chain, 2 kDa isoform; Factor VIIIa heavy chain, 92 kDa isoform; Factor VIII B chain; Factor VIIIa light chain]
TRINITY_DN26379_c8_g1_i1	-2.935813	0.6127	
TRINITY_DN235269_c_g1_i3	-2.932911	0.1264384	Interleukin enhancer-binding factor 3
TRINITY_DN257513_c11_g1_i8	-2.918426	0.1659974	
TRINITY_DN263826_c1_g1_i4	-2.913179	0.213955	
TRINITY_DN247444_c8_g2_i1	-2.911235	0.4524941	Fucolectin-5
TRINITY_DN23722_c2_g1_i4	-2.886393	0.8597915	
TRINITY_DN227492_c_g1_i7	-2.853139	0.162554	
TRINITY_DN2674_c15_g1_i1	-2.849319	0.2737666	
TRINITY_DN2659_c4_g1_i2	-2.844426	0.9483869	
TRINITY_DN267198_c2_g1_i14	-2.831474	0.3426583	
TRINITY_DN259593_c2_g1_i3	-2.769593	1.71E-01	
TRINITY_DN246482_c1_g1_i2	-2.765169	0.4479232	
TRINITY_DN2567_c_g1_i1	-2.763664	0.934368	Chitinase 1 (EC 3.2.1.14)
TRINITY_DN265143_c2_g1_i5	-2.757249	0.122633	
TRINITY_DN26442_c6_g1_i4	-2.73554	0.462975	TBC1 domain family member 9B
TRINITY_DN266734_c2_g1_i2	-2.731927	0.4311518	
TRINITY_DN242729_c1_g1_i3	-2.731398	0.697731	
TRINITY_DN23679_c_g1_i15	-2.713852	0.889283	
TRINITY_DN228261_c5_g2_i6	-2.699353	0.92183	
TRINITY_DN247937_c4_g1_i1	-2.697317	0.329677	Carboxypeptidase A2 (EC 3.4.17.15)
TRINITY_DN262215_c2_g2_i3	-2.688817	0.45931	
TRINITY_DN25982_c_g1_i3	-2.683629	6.82E-01	Leukocyte receptor cluster member 9
TRINITY_DN25689_c_g1_i1	-2.678217	0.228948	Probable RNA-directed DNA polymerase from transposon X-element (EC 2.7.7.49) (Reverse transcriptase)
TRINITY_DN259651_c2_g2_i9	-2.676383	0.1546857	

TRINITY_DN18992_c_g1_i2	-2.668471	0.1277591	
TRINITY_DN23722_c2_g1_i5	-2.662294	0.9278747	
TRINITY_DN251122_c3_g2_i8	-2.65796	0.3124318	
TRINITY_DN237928_c5_g2_i16	-2.647575	0.669929	
TRINITY_DN233877_c_g1_i1	-2.637789	0.2777819	Hybrid PKS-NRPS synthetase lepA (EC 2.3.1.-) (EC 6.3.2.-) (Leporins biosynthesis protein A)
TRINITY_DN23679_c_g1_i1	-2.637236	0.598252	
TRINITY_DN242729_c1_g1_i1	-2.637162	0.169997	Uncharacterized protein CXorf65 homolog
TRINITY_DN262215_c2_g2_i12	-2.598741	0.45931	
TRINITY_DN199613_c2_g1_i2	-2.598713	0.1318118	
TRINITY_DN2689_c9_g1_i4	-2.583317	0.245788	
TRINITY_DN26472_c1_g1_i7	-2.577491	0.8879765	
TRINITY_DN258285_c5_g1_i1	-2.561833	0.6586213	
TRINITY_DN262521_c_g1_i2	-2.559196	0.9322646	
TRINITY_DN267913_c24_g2_i2	-2.548842	0.1876383	Cytochrome P45 27C1 (EC 1.14.19.-) (All-trans retinol 3,4-desaturase)
TRINITY_DN267913_c22_g1_i1	-2.541196	4.86E-01	
TRINITY_DN29389_c2_g1_i1	-2.534716	0.3367941	
TRINITY_DN2629_c_g1_i1	-2.531961	4.40E-01	
TRINITY_DN262819_c2_g1_i5	-2.525123	0.1621768	
TRINITY_DN235269_c_g1_i7	-2.515146	0.4432695	
TRINITY_DN254444_c_g1_i3	-2.497962	1.70E-01	
TRINITY_DN267913_c22_g1_i2	-2.492495	0.75729	25-hydroxyvitamin D-1 alpha hydroxylase, mitochondrial (EC 1.14.15.18) (25-OHD-1 alpha-hydroxylase) (25-hydroxyvitamin D(3) 1-alpha-hydroxylase) (VD3 1A hydroxylase) (Calcidiol 1-monooxygenase) (Cytochrome P45 subfamily XXVIIB polypeptide 1) (Cytochrome P45C1 alpha) (Cytochrome P45VD1-alpha) (Cytochrome p45 27B1)
TRINITY_DN259585_c2_g1_i1	-2.486323	0.223732	Docking protein 3 (Downstream of tyrosine kinase 3)
TRINITY_DN15173_c_g1_i1	-2.483226	0.897533	

TRINITY_DN199613_c2_g1_i1	-2.479975	0.3479	
TRINITY_DN16812_c_g1_i1	-2.478237	6.95E-01	
TRINITY_DN23679_c_g1_i9	-2.475648	0.5295387	
TRINITY_DN23722_c2_g1_i1	-2.473617	0.5886486	
TRINITY_DN2172_c_g1_i1	-2.471578	0.4826689	Four-domain proteases inhibitor (McaPI)
TRINITY_DN266843_c2_g2_i13	-2.468853	0.2321292	
TRINITY_DN23297_c_g1_i2	-2.467277	0.3462317	Fucolectin-1
TRINITY_DN23722_c2_g1_i3	-2.455612	0.1281626	
TRINITY_DN8867_c_g1_i1	-2.453429	0.143291	Tenellin synthetase (TENS) (EC 2.3.1.-) (EC 6.3.2.-) (Hybrid PKS-NRPS synthetase tenS) (Tenellin biosynthesis protein S)
TRINITY_DN24824_c4_g2_i3	-2.453232	8.79E-01	Cytochrome P45 11B, mitochondrial (CYPXIB) (Cytochrome P45C11) (P-45(11 beta,aldo)) (Steroid 11-beta-hydroxylase) (EC 1.14.15.4)
TRINITY_DN157266_c_g1_i1	-2.434898	0.386776	
TRINITY_DN234775_c2_g3_i1	-2.429684	0.2336461	
TRINITY_DN19366_c_g1_i6	-2.42164	0.4423971	
TRINITY_DN253966_c_g1_i6	-2.398963	0.4321331	
TRINITY_DN259593_c2_g1_i4	-2.369594	8.60E-01	
TRINITY_DN245334_c1_g2_i5	-2.369452	0.3871418	
TRINITY_DN26543_c3_g1_i2	-2.368239	0.1338255	
TRINITY_DN247397_c_g1_i1	-2.358752	0.3795744	Agrin [Cleaved into: Agrin N-terminal 11 kDa subunit; Agrin C-terminal 11 kDa subunit; Agrin C-terminal 9 kDa fragment (C9); Agrin C-terminal 22 kDa fragment (C22)]
TRINITY_DN237928_c5_g2_i2	-2.351644	0.6285	
TRINITY_DN267913_c24_g1_i1	-2.338671	3.56E-01	
TRINITY_DN191766_c_g1_i1	-2.331162	0.5313851	
TRINITY_DN25889_c2_g2_i7	-2.321373	0.3666435	Sushi, von Willebrand factor type A, EGF and pentraxin domain-containing protein 1 (Polydom)
TRINITY_DN246482_c1_g1_i1	-2.314513	0.355375	
TRINITY_DN228261_c5_g2_i2	-2.314479	0.418195	Probable cytochrome P45 31a1, mitochondrial (EC 1.14.-.-) (CYPCCCIA1)

Table 7B

Domain Names	log2FoldChange	padj	Annotations
TRINITY_DN26546_c9_g3_i1	7.676841	0.328859	Dual oxidase 1 (EC 1.11.1.-) (EC 1.6.3.1)
TRINITY_DN26546_c9_g2_i4	7.6525758	0.1357448	Eosinophil peroxidase (EPO) (EC 1.11.1.7) [Cleaved into: Eosinophil peroxidase light chain; Eosinophil peroxidase heavy chain]
TRINITY_DN254387_c2_g1_i1	7.4494173	0.263545	
TRINITY_DN22495_c2_g1_i3	7.1954553	0.2533278	Peroxidasin homolog (EC 1.11.1.7)
TRINITY_DN25529_c_g3_i2	6.6431916	0.4186315	
TRINITY_DN239_c_g2_i1	6.4685858	0.1741215	
TRINITY_DN49732_c_g1_i1	6.2427945	0.669763	
TRINITY_DN264398_c1_g1_i1	5.9137939	0.2747586	
TRINITY_DN254583_c4_g2_i1	5.8157293	0.1422943	CD29 antigen (Dendritic cell-specific ICAM-3-grabbing non-integrin 1) (DC-SIGN1) (CD antigen CD29)
TRINITY_DN25171_c_g2_i3	5.747195	0.922689	Methionine synthase (EC 2.1.1.-) (Homocysteine methyltransferase)
TRINITY_DN26726_c5_g4_i2	5.6743541	0.13628	
TRINITY_DN26619_c7_g2_i1	5.5919321	0.5383169	Uromodulin (Tamm-Horsfall urinary glycoprotein) (THP) [Cleaved into: Uromodulin, secreted form]
TRINITY_DN254387_c2_g1_i2	5.5777881	8.45E-01	
TRINITY_DN267918_c114_g1_i2	5.562869	0.4133	
TRINITY_DN265125_c3_g1_i2	5.5196972	0.89345	
TRINITY_DN254583_c4_g2_i4	5.4614954	0.2772928	C-type lectin domain family 4 member M (CD29 antigen-like protein 1) (CD antigen CD299)
TRINITY_DN264398_c1_g1_i3	5.1537458	0.5259964	
TRINITY_DN257934_c1_g2_i1	4.9165996	0.86559	Beta,beta-carotene 15,15'-dioxygenase (EC 1.13.11.63) (Beta-carotene dioxygenase 1) (Beta-carotene oxygenase 1)

TRINITY_DN257934_c1_g1_i2	4.8935858	0.198388	Beta,beta-carotene 9',1'-oxygenase (EC 1.13.11.71) (B-diox-II) (Beta-carotene dioxygenase 2)
TRINITY_DN243845_c_g3_i3	4.8923347	0.2539557	
TRINITY_DN127349_c4_g1_i1	4.8329366	0.467943	
TRINITY_DN247444_c7_g1_i1	4.8122495	0.84451	Retinoid isomerohydrolase (EC 3.1.1.64) (All-trans-retinylester 11-cis isomerohydrolase A) (Meso-zeaxanthin isomerase) (EC 5.3.3.-) (Retinal pigment epithelium-specific 65 kDa protein homolog A) (RPE56a)
TRINITY_DN265125_c3_g1_i4	4.729879	0.2733164	
TRINITY_DN254583_c4_g1_i4	4.588688	0.371297	
TRINITY_DN254583_c4_g1_i3	4.5423718	0.964976	
TRINITY_DN257934_c1_g1_i5	4.5353182	0.492531	
TRINITY_DN258126_c2_g6_i2	4.4775254	0.193214	
TRINITY_DN242189_c_g1_i2	4.4496269	0.2521259	Retinoid isomerohydrolase (EC 3.1.1.64) (All-trans-retinyl-palmitate hydrolase) (Meso-zeaxanthin isomerase) (EC 5.3.3.-) (Retinal pigment epithelium-specific 65 kDa protein) (Retinol isomerase)
TRINITY_DN261341_c4_g1_i2	4.4432839	0.253952	
TRINITY_DN242189_c_g1_i3	4.4222644	0.2336471	
TRINITY_DN22847_c8_g1_i3	4.3416575	0.1373987	
TRINITY_DN24817_c7_g1_i1	4.2298639	4.62E-01	
TRINITY_DN261341_c4_g1_i4	4.167892	0.587655	
TRINITY_DN261244_c3_g1_i7	3.9776777	0.4397	
TRINITY_DN254583_c4_g2_i3	3.9298177	0.2484888	Perlucin-like protein
TRINITY_DN266559_c2_g1_i2	3.9237174	0.73837	Membrane metallo-endopeptidase-like 1 (EC 3.4.24.11) (Membrane metallo-endopeptidase-like 2) (NEP2(m)) (Neprilysin II) (NEPII) (Neprilysin-2) (NEP2) (NL2) [Cleaved into: Membrane metallo-endopeptidase-like 1, soluble form (Neprilysin-2 secreted) (NEP2(s))]
TRINITY_DN237644_c1_g1_i2	3.8975344	0.924	Photosystem I P7 chlorophyll a apoprotein A1 (EC 1.97.1.12) (PSI-A) (PsaA)

TRINITY_DN249328_c9_g1_i1	3.8881526	0.421363	
TRINITY_DN254461_c1_g1_i3	3.8493343	0.198388	Serine/arginine-rich splicing factor 4 (Splicing factor, arginine/serine-rich 4)
TRINITY_DN255933_c2_g2_i11	3.8415817	0.4353986	
TRINITY_DN254737_c4_g5_i2	3.8398855	0.454581	
TRINITY_DN266559_c2_g1_i6	3.829333	0.311373	
TRINITY_DN261341_c3_g1_i4	3.8262189	0.371984	
TRINITY_DN24817_c7_g3_i1	3.8261648	6.78E-01	
TRINITY_DN24817_c7_g1_i4	3.8222831	1.19E-01	
TRINITY_DN27844_c_g1_i1	3.795181	8.97E-01	
TRINITY_DN26726_c5_g2_i3	3.7928715	0.2952756	
TRINITY_DN265864_c6_g3_i1	3.7799743	0.6285	
TRINITY_DN251165_c5_g2_i1	3.7776587	0.224283	
TRINITY_DN263654_c5_g2_i1	3.7745277	0.221968	
TRINITY_DN225982_c_g1_i6	3.7498914	0.5273859	
TRINITY_DN267918_c114_g1_i1	3.7487112	0.598252	
TRINITY_DN25729_c6_g1_i3	3.7342426	0.1174847	Transcription factor Spi-C
TRINITY_DN26337_c6_g2_i2	3.7124286	0.7171931	
TRINITY_DN264129_c3_g1_i12	3.6854352	0.2815941	
TRINITY_DN257232_c4_g1_i8	3.6452684	0.7147979	
TRINITY_DN24778_c2_g1_i2	3.6188425	0.3461598	
TRINITY_DN25339_c3_g1_i8	3.6133614	0.2646561	
TRINITY_DN226453_c_g1_i1	3.538624	0.4212688	
TRINITY_DN159515_c1_g1_i2	3.5128254	0.4642433	
TRINITY_DN26872_c1_g2_i1	3.4757363	0.228768	
TRINITY_DN249414_c1_g5_i2	3.4529262	0.492531	
TRINITY_DN247675_c3_g3_i1	3.4476395	0.1172147	
TRINITY_DN261341_c3_g1_i8	3.4449567	0.614955	
TRINITY_DN254461_c1_g1_i13	3.4167128	0.35732	
TRINITY_DN248855_c1_g4_i1	3.3932499	4.80E-01	

TRINITY_DN242212_c9_g1_i1	3.3914614	0.2214422	
TRINITY_DN1525_c_g1_i1	3.3851455	0.2519663	
TRINITY_DN25171_c_g2_i5	3.3757679	0.1432392	
TRINITY_DN26665_c3_g7_i1	3.3159533	0.1674919	
TRINITY_DN248727_c_g1_i4	3.2967682	0.131993	
TRINITY_DN24778_c2_g1_i3	3.2875148	0.26828	
TRINITY_DN181553_c_g1_i1	3.2798685	0.112292	
TRINITY_DN182745_c_g1_i2	3.2796974	0.3616268	
TRINITY_DN26476_c3_g1_i1	3.2516218	0.168933	
TRINITY_DN26337_c6_g2_i7	3.2352918	0.1899498	
TRINITY_DN264332_c3_g3_i2	3.2347764	0.3378466	
TRINITY_DN25635_c_g3_i1	3.2322266	0.133117	
TRINITY_DN25171_c_g2_i2	3.2293216	0.854392	Methionine synthase (EC 2.1.1.-) (Homocysteine methyltransferase)
TRINITY_DN262173_c_g2_i1	3.1969126	0.1127388	
TRINITY_DN266559_c2_g1_i3	3.1955625	0.359298	
TRINITY_DN265991_c5_g2_i8	3.1881532	0.386729	
TRINITY_DN252344_c12_g2_i3	3.1696973	0.344931	
TRINITY_DN244989_c_g1_i2	3.1314456	0.2642	
TRINITY_DN25729_c6_g1_i1	3.1277483	0.174614	
TRINITY_DN25171_c_g2_i4	3.1232368	0.3391194	
TRINITY_DN25729_c6_g1_i8	3.1162372	0.434942	
TRINITY_DN244989_c_g1_i1	3.1127458	0.61698	
TRINITY_DN253469_c1_g1_i1	3.1118723	0.636493	PI-PLC X domain-containing protein 3
TRINITY_DN266469_c_g1_i1	2.9972179	0.6446152	E3 ubiquitin-protein ligase TRIM56 (EC 2.3.2.27) (RING-type E3 ubiquitin transferase TRIM56) (Tripartite motif-containing protein 56)
TRINITY_DN23871_c1_g1_i4	2.9941325	0.416599	
TRINITY_DN247822_c_g2_i5	2.9849127	0.37236	
TRINITY_DN257934_c1_g1_i3	2.984472	0.217497	
TRINITY_DN22392_c_g1_i1	2.9786145	0.981938	

TRINITY_DN256372_c5_g2_i5	2.9748873	0.6789682	
TRINITY_DN25452_c_g1_i1	2.965196	0.6444722	
TRINITY_DN28666_c_g1_i1	2.9584689	0.4397	Techylectin-5A
TRINITY_DN262327_c3_g1_i8	2.9583769	0.777378	Myb-related protein A (A-Myb) (Myb-like protein 1)
TRINITY_DN249967_c_g1_i1	2.9448588	0.619439	
TRINITY_DN25769_c_g2_i1	2.944324	0.1674919	

TABLE 7: Control vs Short Term Heat Stress DEG Results. Pairwise analysis ($p<0.05$) was performed on samples with normal temperatures and an elevated temperature (34° C) for a period of 12 hours in EL1 infected *Cassiopea*. Genes were sorted based on decreasing magnitudes of log2FoldChanges. **A.** Down-regulated genes and their differential expression values. **B.** Up-regulated genes and their differential values.

REFERENCES

Abram, N. J., McGregor, H. V., Tierney, J. E., Evans, M. N., McKay, N. P., Kaufman, D. S., . . . Kvartärgeologi. (2016). Early onset of industrial-era warming across the oceans and continents. *Nature, 536*(7617), 411-418. doi:10.1038/nature19082

Allison, S. (2017). Uromodulin in ER stress and apoptosis. *Nature Reviews Nephrology, 13*(12) doi:10.1038/nrneph.2017.152

Aruda, A. M., Baumgartner, M. F., Reitzel, A. M., & Tarrant, A. M. (2011). Heat shock protein expression during stress and diapause in the marine copepod calanus finmarchicus. *Journal of Insect Physiology, 57*(5), 665-675. doi:10.1016/j.jinsphys.2011.03.007

Bay, R. A., & Palumbi, S. R. (2017). Transcriptome predictors of coral survival and growth in a highly variable environment. *Ecology and evolution, 7*(13), 4794-4803.

Benjamin, I. J., & McMillan, D. R. (1998). Stress (heat shock) proteins: Molecular chaperones in cardiovascular biology and disease. *Circulation Research, 83*(2), 117-132. doi:10.1161/01.RES.83.2.117

Bultynck, G., Heath, V. L., Majeed, A. P., Galan, J., Haguenauer-Tsapis, R., & Cyert, M. S. (2006). Slm1 and Slm2 are novel substrates of the calcineurin phosphatase required for heat stress-induced endocytosis of the yeast uracil permease. *Molecular and Cellular Biology, 26*(12), 4729-4745. doi:10.1128/MCB.01973-05

Cabrales-Arellano, P., Islas-Flores, T., Thomé, P. E., & Villanueva, M. A. (2017). Indomethacin reproducibly induces metamorphosis in cassiopea xamachana scyphistomae. *Peerj, 5*, e2979. doi:10.7717/peerj.2979

Chen, H., Wen, Q., Wang, W., He, J., & Wu, Q. (2013). The orphan nuclear receptor TR3/Nur77 regulates ER stress and induces apoptosis via interaction with TRAP gamma. *International Journal of Biochemistry & Cell Biology, 45*(8), 1600-1609. doi:10.1016/j.biocel.2013.04.026

Chen, P., Fonseca, L., Hannun, Y., & Voit, E. (2013). Coordination of rapid sphingolipid responses to heat stress in yeast. *Plos Computational Biology, 9*(5), e1003078. doi:10.1371/journal.pcbi.1003078

Chitin: TAKENAKA, Y., NAKANO, S., TAMOI, M., SAKUDA, S., & FUKAMIZO, T. (2009). Chitinase gene expression in response to environmental stresses in arabidopsis thaliana: Chitinase inhibitor allosamidin enhances stress tolerance. *Bioscience, Biotechnology, and Biochemistry, 73*(5), 1066-1071. doi:10.1271/bbb.80837

Clark, M. S., Keiron P. P. Fraser, & Peck, L. S. (2008). Antarctic marine molluscs do have an HSP70 heat shock response. *Cell Stress & Chaperones, 13*(1), 39-49. doi:10.1007/s12192-008-0014-8

Cold stress adaptation: Kim, J. S., Park, S. J., Kwak, K. J., Kim, Y. O., Kim, J. Y., Song, J., ... & Kang, H. (2006). Cold shock domain proteins and glycine-rich RNA-binding proteins from Arabidopsis thaliana can promote the cold adaptation process in Escherichia coli. *Nucleic Acids Research*, *35*(2), 506-516.

CYTOCHROM 450 이동욱, & 박기현. (1990). Poster III : Characterization of cytochrome P -450 degradation by oxidative stress. *90 년도 학술대회 초록*, , 99.

Davy, S. K., Allemand, D., & Weis, V. M. (2012). Cell biology of cnidarian-dinoflagellate symbiosis. *Microbiology and Molecular Biology Reviews, 76*(2), 229-261.

doi:10.1104/pp.16.00648 (Fujikane et al. 2016)

DeSalvo, M. K., Voolstra, C. R., Sunagawa, S., Schwarz, J. A., Stillman, J. H., Coffroth, M. A., ... & Medina, M. (2008). Differential gene expression during thermal stress and bleaching in the Caribbean coral Montastraea faveolata. *Molecular ecology, 17*(17), 3952-3971.

DeSalvo, M. K., Sunagawa, S., Fisher, P. L., Voolstra, C. R., IGLESIAS-PRIETO, R., & Medina, M. (2010). Coral host transcriptomic states are correlated with Symbiodinium genotypes. *Molecular ecology*, *19*(6), 1174-1186.

Donner, S. D., Skirving, W. J., Little, C. M., Oppenheimer, M., & Hoegh-Guldberg, O. V. E. (2005). Global assessment of coral bleaching and required rates of adaptation under climate change. *Global Change Biology*, *11*(12), 2251-2265.

Dunlop, R. A., Powell, J. T., Metcalf, J. S., Guillemin, G. J., & Cox, P. A. (2018). l-serine-mediated neuroprotection includes the upregulation of the ER stress chaperone protein disulfide isomerase (PDI). *Neurotoxicity Research, 33*(1), 113-122. doi:10.1007/s12640-017-9817-7

Dwivedi, R. S., Breiman, A., & Herman, E. M. (2003). Differential distribution of the cognate and heat-stress-induced isoforms of high mr cis-trans prolyl peptidyl isomerase (FKBP) in the cytoplasm and nucleoplasm. *Journal of Experimental Botany, 54*(393), 2679-2689. doi:10.1093/jxb/erg307

E3 ubiquitin: Yan, J., Wang, J., Li, Q., Hwang, J. R., Patterson, C., & Zhang, H. (2003). AtCHIP, a U-box-containing E3 ubiquitin ligase, plays a critical role in temperature stress tolerance in Arabidopsis. *Plant Physiology*, *132*(2), 861-869.

Endo, S., Matsunaga, T., Mamiya, H., Hara, A., Kitade, Y., Tajima, K., & El-Kabbani, O. (2009). Characterization of a rat NADPH-dependent aldo-keto reductase (AKR1B13) induced by oxidative stress. *Chemico-Biological Interactions, 178*(1), 151-157. doi:10.1016/j.cbi.2008.09.010

Eskandani, M., Golchai, J., Pirooznia, N., & Hasannia, S. (2010). Oxidative stress level and tyrosinase activity in vitiligo patients. *Indian journal of dermatology*, *55*(1), 15.

Fan, L., Liu, M., Simister, R., Webster, N. S., & Thomas, T. (2013). Marine microbial symbiosis heats up: The phylogenetic and functional response of a sponge holobiont to thermal stress. *The ISME Journal, 7*(5), 991. doi:10.1038/ismej.2012.165f

Fan, T., Wang, R., Xiang, Y., An, L., & Cao, S. (2016). Heat stress induces actin cytoskeletal reorganization and transcript profiles of vegetative profilins and actin depolymerizing factors (ADFs) in arabidopsis. *Acta Physiologiae Plantarum, 38*(2), 1-4. doi:10.1007/s11738-016-2061-6

Fisher, G. J., Quan, T., Purohit, T., Shao, Y., Cho, M. K., He, T., . . . Voorhees, J. J. (2009). Collagen fragmentation promotes oxidative stress and elevates matrix metalloproteinase-1 in fibroblasts in aged human skin. *American Journal of Pathology, 174*(1), 101-114. doi:10.2353/ajpath.2009.080599

Fujikane, R., Komori, K., Sekiguchi, M., & Hidaka, M. (2016). Function of high-mobility group A proteins in the DNA damage signaling for the induction of apoptosis. *Scientific Reports, 6*, 31714-31714. doi:10.1038/srep31714

Giri, J., Vij, S., Dansana, P. K., & Tyagi, A. K. (2011). Rice A20/AN1 zinc-finger containing stress-associated proteins (SAP1/11) and a receptor-like cytoplasmic kinase (OsRLCK253) interact via A20 zinc-finger and confer abiotic stress tolerance in transgenic arabidopsis plants. *The New Phytologist, 191*(3), 721-732. doi:10.1111/j.1469-8137.2011.03740.x

Gössling, S., Hall, C. M., Peeters, P., & Scott, D. (2010). The future of tourism: Can tourism growth and climate policy be reconciled? A mitigation perspective. *Tourism Recreation Research, 35*(2), 119-130.

He, T., Quan, T., Voorhees, J., & Fisher, G. (2015). Oxidative stress reduces collagen production through eIF2 alpha-dependent down-regulation of transforming growth factor-beta signaling pathway in human dermal fibroblasts. Paper presented at the , *135* S84-S84.

Heat shock protein 7 Chan, Y., Greenwood, D., Yang, Y., Leung, E., & Krissansen, G. (2015). Leukocyte integrin alpha 4 beta 7 associates with heat shock protein 70. *Molecular and Cellular Biochemistry, 409*(1-2), 263-269. doi:10.1007/s11010-015-2530-z

Heat shock protein 70 Zhang, Q., & Denlinger, D. L. (2010). Molecular characterization of heat shock protein 90, 70 and 70 cognate cDNAs and their expression patterns during thermal stress and pupal diapause in the corn earworm. *Journal of Insect Physiology, 56*(2), 138-150. doi:10.1016/j.jinsphys.2009.09.013

Hoegh-Guldberg, O. (1999). Climate change, coral bleaching and the future of the world's coral reefs. *Marine and freshwater research, 50*(8), 839-866.

Hoegh-Guldberg, O., & Bruno, J. F. (2010). The impact of climate change on the world's marine ecosystems. *Science, 328*(5985), 1523-1528. doi:10.1126/science.1189930

Hoegh-Guldberg, O., Mumby, P. J., Hooten, A. J., Steneck, R. S., Greenfield, P., Gomez, E., . . . Hatziolos, M. E. (2007). Coral reefs under rapid climate change and ocean acidification. *Science, 318*(5857), 1737-1742. doi:10.1126/science.1152509

Hondorp, E., & Matthews, R. (2004). Oxidative stress inactivates cobalamin-independent methionine synthase (MetE) in escherichia coli. *Plos Biology, 2*(11), 1738-1753. doi:10.1371/journal.pbio.0020336'

Hong, F., Lee, J., Song, J., Lee, S. J., Ahn, H., Cho, J. J., . . . Kim, S. S. (2002). Cyclosporin A blocks muscle differentiation by inducing oxidative stress and inhibiting the peptidyl-prolyl-cis-trans isomerase activity of cyclophilin A: Cyclophilin A protects myoblasts from cyclosporin A-induced cytotoxicity. *FASEB Journal : Official Publication of the Federation of American Societies for Experimental Biology, 16*(12), 1633.

Huang, Z., Zhou, M., Wang, Q., Zhu, M., Chen, S., & Li, H. (2017). Mechanical and hypoxia stress can cause chondrocytes apoptosis through over-activation of endoplasmic reticulum stress. *Archives of Oral Biology, 84*, 125-132. doi:10.1016/j.archoralbio.2017.09.021

Hume, B., D'Angelo, C., Burt, J., Baker, A. C., Riegl, B., & Wiedenmann, J. (2013). Corals from the Persian/Arabian gulf as models for thermotolerant reef-builders: Prevalence of clade C3 symbiodinium, host fluorescence and ex situ temperature tolerance. *Marine Pollution Bulletin, 72*(2), 313-322. doi:10.1016/j.marpolbul.2012.11.032

IPCC, Climate Change 2007: The Physical Science Basis. Contribution of Working Group I to the Fourth Assessment Report of the Intergovernmental Panel on Chmate Change, S. Solomon et ai, Eds. (Cambridge Univ. Press, Cambridge, UK, and New York, 2007)

Jones, G. P., McCormick, M. I., Srinivasan, M., & Eagle, J. V. (2004). Coral decline threatens fish biodiversity in marine reserves. *Proceedings of the National Academy of Sciences of the United States of America, 101*(21), 8251-8253.

Kannan, K., & Jain, S. K. (2000). Oxidative stress and apoptosis. *Pathophysiology, 7*(3), 153-163.

Kasperczyk, S., Dobrakowski, M., Kasperczyk, J., Ostalowska, A., Zalejska-Fiolka, J., & Birkner, E. (2014). Beta-carotene reduces oxidative stress, improves glutathione metabolism and modifies antioxidant

defense systems in lead-exposed workers. *Toxicology and Applied Pharmacology, 280*(1), 36-41. doi:10.1016/j.taap.2014.07.006

Kim, J. Y., Park, S. J., Jang, B., Jung, C. H., Ahn, S. J., Goh, C. H., ... & Kang, H. (2007). Functional characterization of a glycine-rich RNA-binding protein 2 in Arabidopsis thaliana under abiotic stress conditions. *The Plant Journal, 50*(3), 439-451. (Kim et al. 2007)

Kim, J., Oh, J., Yoon, D., & Sung, G. (2017). Suppression of a methionine synthase by calmodulin under environmental stress in the entomopathogenic fungus beauveria bassiana. *Environmental Microbiology Reports, 9*(5), 612-617. doi:10.1111/1758-2229.12548

Kim, Y., Lee, H., Manson, S., Lindahl, M., Evans, B., Miner, J., . . . Chen, Y. (2016). Mesencephalic astrocyte-derived neurotrophic factor as a urine biomarker for endoplasmic reticulum stress-related kidney diseases. *Journal of the American Society of Nephrology, 27*(10), 2974-2982. doi:10.1681/ASN.2014100986

King, A. M., & MacRae, T. H. (2015). Insect heat shock proteins during stress and diapause. *Annual Review of Entomology, 60*(1), 59-75. doi:10.1146/annurev-ento-011613-162107

Kotak, S., Larkindale, J., Lee, U., von Koskull-Döring, P., Vierling, E., & Scharf, K. (2007). Complexity of the heat stress response in plants. *Current Opinion in Plant Biology, 10*(3), 310-316. doi:10.1016/j.pbi.2007.04.011, Mittler, R., Finka, A., & Goloubinoff, P. (2012). How do plants feel the heat? *Trends in Biochemical Sciences, 37*(3), 118-125. doi:10.1016/j.tibs.2011.11.007).

Kumar, S., Singh, R., Williams, C. P., & van der Klei, Ida J. (2016). Stress exposure results in increased peroxisomal levels of yeast Pnc1 and Gpd1, which are imported via a piggy-backing mechanism. *Biochimica Et Biophysica Acta, 1863*(1), 148.

Ladner, J. T., Barshis, D. J., & Palumbi, S. R. (2012). Protein evolution in two co-occurring types of Symbiodinium: an exploration into the genetic basis of thermal tolerance in Symbiodinium clade D. *BMC evolutionary biology, 12*(1), 217.

LaJeunesse, T. C., Wham, D. C., Pettay, D. T., Parkinson, J. E., Keshavmurthy, S., & Chen, C. A. (2014). Ecologically differentiated stress-tolerant endosymbionts in the dinoflagellate genus symbiodinium (dinophyceae) clade D are different species. *Phycologia, 53*(4), 305.

Leśniak, W., Szczepańska, A., & Kuźnicki, J. (2005). Calcyclin (S100A6) expression is stimulated by agents evoking oxidative stress via the antioxidant response element. *Biochimica et Biophysica Acta (BBA)-Molecular Cell Research, 1744*(1), 29-37.

Levin, R. A., Beltran, V. H., Hill, R., Kjelleberg, S., McDougald, D., Steinberg, P. D., & van Oppen, M. J. (2016). Sex, scavengers, and chaperones: transcriptome secrets of divergent Symbiodinium thermal tolerances. *Molecular biology and evolution, 33*(9), 2201-2215.

Lien, Y., Fukami, H., & Yamashita, Y. (2013). Genetic variations within symbiodinium clade C among zooxanthellate corals (scleractinia) in the temperate zone of japan. *Fisheries Science, 79*(4), 579-591. doi:10.1007/s12562-013-0623-8 – diversity within clade c

Lin, Z., Chen, M., Dong, X., Zheng, X., Huang, H., Xu, X., & Chen, J. (2017). Transcriptome profiling of Galaxea fascicularis and its endosymbiont Symbiodinium reveals chronic eutrophication tolerance pathways and metabolic mutualism between partners. *Scientific reports, 7*, 42100.

Mann, M. E., Zhang, Z., Hughes, M. K., Bradley, R. S., Miller, S. K., Rutherford, S., & Ni, F. (2008). Proxy-based reconstructions of hemispheric and global surface temperature variations over the past two

millennia. *Proceedings of the National Academy of Sciences of the United States of America, 105*(36), 13252-13257. doi:10.1073/pnas.0805721105

Maor-Landaw, K., & Levy, O. (2016). Gene expression profiles during short-term heat stress; branching vs. massive scleractinian corals of the red sea. *Peerj, 4*, e1814. doi:10.7717/peerj.1814

Menike, U., Lee, Y., Oh, C., Wickramaarachchi, W. D. N., Premachandra, H. K. A., Park, S. C., . . . De Zoysa, M. (2014). Oligo-microarray analysis and identification of stress-immune response genes from manila clam (ruditapes philippinarum) exposure to heat and cold stresses. *Molecular Biology Reports, 41*(10), 6457-6473. doi:10.1007/s11033-014-3529-3

Menzel, A., Sparks, T., Estrella, N., Koch, E., Aasa, A., Ahas, R., . . . Institutionen för växt- och miljövetenskaper. (2006). European phenological response to climate change matches the warming pattern. *Global Change Biology, 12*(10), 1969-1976. doi:10.1111/j.1365-2486.2006.01193.x

Muras, V., Dogaru-Kinn, P., Minato, Y., Hase, C., & Steuber, J. (2016). The na+-translocating NADH: Quinone oxidoreductase enhances oxidative stress in the cytoplasm of vibrio cholerae. *Journal of Bacteriology, 198*(17), 2307-2317. doi:10.1128/JB.00342-16

Narusaka, M., Seki, M., Umezawa, T., Ishida, J., Nakajima, M., Enju, A., & Shinozaki, K. (2004). Crosstalk in the responses to abiotic and biotic stresses in Arabidopsis: analysis of gene expression in cytochrome P450 gene superfamily by cDNA microarray. *Plant molecular biology*, *55*(3), 327-342.

Nebert, D. W., & Russell, D. W. (2002). Clinical importance of the cytochromes P450. *The Lancet*, *360*(9340), 1155-1162.

Neta-Sharir, I., Isaacson, T., Lurie, S., & Weiss, D. (2005). Dual role for tomato heat shock protein 21: protecting photosystem II from oxidative stress and promoting color changes during fruit maturation. *The Plant Cell*, *17*(6), 1829-1838.

Nishiuchi, T. (2013). Plant Response to Fusarium Metabolites. *Fusarium: genomics, molecular and cellular biology*, 165-178

Olsen, K., Ritson-Williams, R., Ochrietor, J. D., Paul, V. J., & Ross, C. (2013). Detecting hyperthermal stress in larvae of the hermatypic coral porites astreoides: The suitability of using biomarkers of oxidative stress versus heat-shock protein transcriptional expression. *Marine Biology, 160*(10), 2609-2618. doi:10.1007/s00227-013-2255-z

Pandey, S., Sharma, A., Tripathi, D., Kumar, A., Khubaib, M., Bhuwan, M., . . . Ehtesham, N. (2016). Mycobacterium tuberculosis peptidyl-prolyl isomerases also exhibit chaperone like activity in-vitro and in-vivo. *Plos One, 11*(3), e0150288. doi:10.1371/journal.pone.0150288

Park, G., & Oh, M. S. (2015). Acceleration of heat shock-induced collagen breakdown in human dermal fibroblasts with knockdown of NF-E2-related factor 2. *BMB Reports, 48*(8), 467-472. doi:10.5483/BMBRep.2015.48.8.215

Park, K., & Kwak, I. (2014). Characterization and gene expression of heat shock protein 90 in marine crab following bisphenol A and 4-nonylphenol exposures. *Environmental Health and Toxicology, 29* doi:10.5620/eht.2014.29.e2014002

Parmesan, C. (2006). Ecological and evolutionary responses to recent climate change. *Annual Review of Ecology, Evolution, and Systematics, 37*(1), 637-669. doi:10.1146/annurev.ecolsys.37.091305.110100

Parmesan, C., & Yohe, G. (2003). A globally coherent fingerprint of climate change impacts across natural systems. *Nature*, *421*(6918), 37.–> introduction of systems problems 42 (2003).

Peptidyl:

Perez, S., & Weis, V. (2006). Nitric oxide and cnidarian bleaching: An eviction notice mediates breakdown of a symbiosis. *The Journal of Experimental Biology, 209*(Pt 14), 2804-2810. doi:10.1242/jeb.02309

Rajan, V. B. V., & D'Silva, P. (2009). Arabidopsis thaliana J-class heat shock proteins: Cellular stress sensors. *Functional & Integrative Genomics, 9*(4), 433-446. doi:10.1007/s10142-009-0132-0

Rasheva, V., & Domingos, P. (2009). Cellular responses to endoplasmic reticulum stress and apoptosis. *Apoptosis, 14*(8), 996-1007. doi:10.1007/s10495-009-0341-y

Rieder, M. J., Carmona, R., Krieger, J. E., Pritchard, K. A. J., & Greene, A. S. (1997). Suppression of angiotensin-converting enzyme expression and activity by shear stress. *Circulation research, 80*(3), 312-319.

Rodriguez-Lanetty, M., Krupp, D., & Weis, V. (2004). Distinct ITS types of symbiodinium in clade C correlate with cnidarian/dinoflagellate specificity during onset of symbiosis. *Marine Ecology Progress Series, 275*, 97-102. doi:10.3354/meps275097

Rodriguez-Serrano, M., Romero-Puertas, M., Sanz-Fernandez, M., Hu, J., & Sandalio, L. (2016). Peroxisomes extend peroxules in a fast response to stress via a reactive oxygen species-mediated induction of the peroxin PEX11a. *Plant Physiology, 171*(3), 1665-1674. (Rodriguez-Serrano et al. 2016)

Root, T. L., Price, J. T., Hall, K. R., Schneider, S. H., Rosenzweig, C., & Pounds, J. A. (2003). Fingerprints of global warming on wild animals and plants. *Nature, 421*(6918), 57.→ speciation patterns

Roth, M. S., & Deheyn, D. D. (2013). Effects of cold stress and heat stress on coral fluorescence in reef-building corals. *Scientific Reports, 3*, 1421. doi:10.1038/srep01421

Saito, K., Kukita, K., Kutomi, G., Okuya, K., Asanuma, H., Tabeya, T., . . . Tamura, Y. (2015). Heat shock protein 90 associates with Toll-like receptors 7/9 and mediates self-nucleic acid recognition in SLE. *European Journal of Immunology, 45*(7), 2028-2041. doi:10.1002/eji.201445293

Salunga, T. L., Cui, Z., Shimoda, S., Zheng, H., Nomoto, K., Kondo, T., . . . Tsuneyama, K. (2007). Oxidative stress-induced apoptosis of bile duct cells in primary biliary cirrhosis. *Journal of Autoimmunity, 29*(2), 78-86. doi:10.1016/j.jaut.2007.04.002

Sandiford, S. D. E., Kennedy, K. A. M., Xie, X., Pickering, J. G., & Li, S. S. C. (2014). Dual oxidase maturation factor 1 (DUOXA1) overexpression increases reactive oxygen species production and inhibits murine muscle satellite cell differentiation. *Cell Communication and Signaling : CCS, 12*(1), 5-5. doi:10.1186/1478-811X-12-5

Schrader, M., & Fahimi, H. D. (2006). Peroxisomes and oxidative stress. *Biochimica et Biophysica Acta (BBA)-Molecular Cell Research, 1763*(12), 1755-1766.

Sebens, K. P. (1994). Biodiversity of coral reefs: what are we losing and why?. *American zoologist, 34*(1), 115-133.

Shen, J., Xiang, X., Chen, L., Wang, H., Wu, L., Sun, Y., . . . Chin, Y. E. (2017). JMJD5 cleaves monomethylated histone H3 N-tail under DNA damaging stress. *EMBO Reports, 18*(12), 2131-2143. doi:10.15252/embr.201743892

Silverstein, R. N., Cunning, R., & Baker, A. C. (2017). Tenacious D: Symbiodinium in clade D remain in reef corals at both high and low temperature extremes despite impairment. *The Journal of Experimental Biology, 220*(7), jeb.148239-1196. doi:10.1242/jeb.148239

Sirtori, L. R., Dutra-Filho, C. S., Fitarelli, D., Sitta, A., Haeser, A., Barschak, A. G., ... & Giugliani, R. (2005). Oxidative stress in patients with phenylketonuria. *Biochimica et Biophysica Acta (BBA)-Molecular Basis of Disease*, *1740*(1), 68-73.

Sonna, L. A., Wenger, C. B., Flinn, S., Sheldon, H. K., Sawka, M. N., & Lilly, C. M. (2004). Exertional heat injury and gene expression changes: A DNA microarray analysis study. *Journal of Applied Physiology*, *96*(5), 1943-1953. doi:10.1152/japplphysiol.00886.2003

Stat, M., Morris, E., & Gates, R. D. (2008). Functional diversity in coral: Dinoflagellate symbiosis. *Proceedings of the National Academy of Sciences of the United States of America*, *105*(27), 9256-9261. doi:10.1073/pnas.0801328105 – Symbiodinium

Stat, M., Morris, E., & Gates, R. D. (2008). Functional diversity in coral–dinoflagellate symbiosis. *Proceedings of the National Academy of Sciences*, *105*(27), 9256-9261.

Takahashi, S., Nakamura, T., Sakamizu, M., van Woesik, R., & Yamasaki, H. (2004). Repair machinery of symbiotic photosynthesis as the primary target of heat stress for reef-building corals. *Plant & Cell Physiology*, *45*(2), 251-255. doi:10.1093/pcp/pch028

Tian, Y., Zhao, G., Fang, W., Xu, Q., & Tan, R. (2015). Delta 10(E)-sphingolipid desaturase involved in fusaruside mycosynthesis and stress adaptation in fusarium graminearum. *Scientific Reports*, *5* doi:10.1038/srep10486

Tran, L. P., Nakashima, K., Sakuma, Y., Osakabe, Y., Qin, F., Simpson, S. D., . . . Yamaguchi-Shinozaki, K. (2007). Co-expression of the stress-inducible zinc finger homeodomain ZFHD1 and NAC transcription factors enhances expression of the ERD1 gene in arabidopsis. *The Plant Journal*, *49*(1), 46-63. doi:10.1111/j.1365-313X.2006.02932.x

Tsai, H. M., Sussman, I. I., & Nagel, R. L. (1994). Shear stress enhances the proteolysis of von Willebrand factor in normal plasma. *Blood*, *83*(8), 2171-2179.

Unfolded protein calreticulun: Vargas, J. A. G. (2016). *Regulation of the signal transduction pathways of the unfolded protein response during chronic and physiological ER stresses*

Wang, W., Vinocur, B., Shoseyov, O., & Altman, A. (2004). Role of plant heat-shock proteins and molecular chaperones in the abiotic stress response. *Trends in plant science*, *9*(5), 244-252.

Wang, Y., Xuan, L., Cui, X., Wang, Y., Chen, S., Wei, C., & Zhao, M. (2017). Ibutilide treatment protects against ER stress induced apoptosis by regulating calumenin expression in tunicamycin treated cardiomyocytes. *Plos One*, *12*(4), e0173469. doi:10.1371/journal.pone.0173469

Weber, M., & Medina, M. (2012). The role of microalgal symbionts (symbiodinium) in holobiont physiology. (pp. 119-140). LONDON: ACADEMIC PRESS LTD-ELSEVIER SCIENCE LTD. doi:10.1016/B978-0-12-391499-6.00004-9

Weis, V. M., Davy, S. K., Hoegh-Guldberg, O., Rodriguez-Lanetty, M., & Pringle, J. R. (2008). Cell biology in model systems as the key to understanding corals. *Trends in ecology & evolution*, *23*(7), 369-376.

Yi, G., Li, L., Luo, M., He, X., Zou, Z., Gu, Z., & Su, L. (2017). Heat stress induces intestinal injury through lysosome- and mitochondria-dependent pathway in vivo and in vitro. *Oncotarget*, *8*(25), 40741-40755. doi:10.18632/oncotarget.16580

Yin, J., Liu, M., Ren, W., Duan, J., Yang, G., Zhao, Y., . . . Yin, Y. (2015). Effects of dietary supplementation with glutamate and aspartate on diquat-induced oxidative stress in piglets. *PloS One, 10*(4), e0122893. doi:10.1371/journal.pone.0122893

Zhang, Y., Zhou, Z., Wang, L., & Huang, B. (2018). Transcriptome, expression, and activity analyses reveal a vital heat shock protein 70 in the stress response of stony coral pocillopora damicornis. *Cell Stress & Chaperones,* , 1-11. doi:10.1007/s12192-018-0883-4Clark, M. S., Keiron P. P. Fraser, & Peck, L. S. (2008). Antarctic marine molluscs do have an HSP70 heat shock response. *Cell Stress & Chaperones, 13*(1), 39-49. doi:10.1007/s12192-008-0014-8